# Paravertebral Brown Adipose Tissue (pBAT): Physiological Role in Thermogenesis


Nafisa Djumaeva

St Hilda's College

University of Oxford

Candidate number: 1751414

*A thesis submitted for the degree of*

*MSc by Research in Physiology, Anatomy and Genetics*

Trinity 2025

# Abstract

Brown adipose tissue (BAT) is a metabolically active organ specialized in dissipating chemical energy as heat through non-shivering thermogenesis, primarily mediated by mitochondrial uncoupling protein 1 (UCP1). Interscapular BAT (iBAT) serves as dominant thermogenic site in infants and small mammals, however in humans it undergoes age-dependent degeneration, leading to the long-standing assumption that BAT-mediated thermogenesis is absent in adults. However, this assumption has since been disproven by positron emission tomography/computed tomography (PET/CT) studies revealing metabolically active BAT depots in adult men. Among these depots is the paravertebral BAT (pBAT) located adjacent to sympathetic ganglia. This project investigates the potential role of pBAT as an active thermogenic tissue, by examining its transcriptional profile and response to thermogenic stimuli, such as cold exposure and β-adrenergic activation. Our findings indicate that pBAT displays a strong thermogenic gene expression signature and could represent a human equivalent or alternative to classical iBAT.

# Acknowledgements

I would like to express my heartfelt gratitude to my parents, aunt and brother for their love and support throughout my academic journey. I also extend my thanks to my supervisors, Professor Ana Domingos, Dr Costas Christodoulides and the Domingos lab (David, Gitalee, Rodrigo, Ji, Samson, Hellen, Charlie, Hanyu) for providing me with the opportunity to pursue this research, encouraging my progress and offering outstanding support.

# Table of Contents

# List of Figures



# List of tables

# List of Abbreviations

| | |
|---|---|
| 18F-FDG PET/CT | 18F-fluorodeoxyglucose positron emission tomography/computed tomography |
| 99mTC-MIBI | Mitochondrial tracer 99mTc-methoxyisobutylisonitrile |
| ANOVA | Analysis of Variance |
| ATGL | Adipose Triglyceride Lipase |
| BAT | Brown Adipose Tissue |
| BeAT | Beige Adipose Tissue |
| β-AR | Beta-Adrenergic (1/2/3) / Beta Adrenergic Receptor |
| cAMP | Cyclic Adenosine Monophosphate |
| CE | Cold-Exposure |
| CEBP | CCAAT/enhancer-binding protein (C/EBP) |
| Cidea | Cell Death-Inducing DFFA-Like Effector A |
| CNS | Central Nervous System |
| CREB | cAMP Response Element-Binding Protein |
| DH | Dorsal Horn |
| DNA | Deoxyribonucleic Acid |
| DMH | Dorsomedial Hypothalamus |
| DRG | Dorsal Root Ganglion |

| | |
|---|---|
| ELOVL3 | Elongation of Very Long Chain Fatty Acids Protein 3 |
| Epi | Epinephrine |
| ETC | Electron Transport Chain |
| FFAs | Free Fatty Acids |
| gWAT | Gonadal White Adipose Tissue |
| Gs | Stimulatory G protein (G-protein subunit alpha-s) |
| HPRT1 | Hypoxanthine Phosphoribosyltransferase 1 |
| HSL | Hormone-Sensitive Lipase |
| iBAT | Interscapular Brown Adipose Tissue |
| IF | Immunofluorescence |
| IML | Intermediolateral Nucleus (spinal cord) |
| KO | Knockout |
| LPBd | Dorsal Subnucleus of Lateral Parabrachial Nucleus |
| LPBel | External Lateral Subnucleus of Lateral Parabrachial Nucleus |
| MnPO | Median Preoptic Nucleus |
| MPO | Medial Preoptic Area |
| NTS | Nucleus of the Solitary Tract |
| NE | Norepinephrine |
| NST | Non-Shivering Thermogenesis |

| | |
|---|---|
| PFA | Paraformaldehyde |
| PBS | Phosphate Buffered Saline |
| Pgc-1α | Peroxisome Proliferator-Activated Receptor Gamma Coactivator 1-alpha |
| PKA | Protein Kinase A |
| PPARγ | Peroxisome Proliferator-Activated Receptor Gamma |
| Prdm16 | PR Domain-Containing 16 |
| PGE2 | Prostaglandin E2 |
| PVH | Paraventricular Hypothalamus |
| qRT-PCR | Quantitative Reverse Transcription Polymerase Chain Reaction |
| rRPa | Rostral Raphe Pallidus |
| RNA | Ribonucleic Acid |
| scWAT | Subcutaneous White Adipose Tissue |
| SEM | Standard Error of the Mean |
| SNA | Sympathetic Nervous Activity |
| SNS | Sympathetic Nervous System |
| TAG | Triacylglycerol |
| TG | Triglycerides |
| TH | Tyrosine Hydroxylase |

| | |
|---|---|
| TN | Thermoneutral |
| TRP | Transient Receptor Potential |
| UCP1 | Uncoupling Protein 1 |
| VGLUT3 | Vesicular Glutamate Transporter 3 |
| vWAT | Visceral White Adipose Tissue |
| WAT | White Adipose Tissue |
| WT | Wild Type |
| W-S neurons | Warm-Sensitive Neurons |
| PeF-LH | Perifornical Lateral Hypothalamus |
| EP3 receptor | Prostaglandin E2 Receptor EP3 subtype |
| POA | Preoptic Area |
| VLM | Ventrolateral Medulla |

# 1

# Introduction

## Contents



## 1.1 Overview of Adipose Tissue

Adipose tissue plays a central role in regulating energy metabolism. Despite the previous belief that it acts solely as passive energy reservoir, vast research has now established its role as a dynamic metabolic organ (Cannon and Nedergaard, 2004; Luo and Liu, 2016). Our understanding was historically limited to white adipose tissue (WAT), the most

abundant type of fat. However, numerous studies have established the heterogeneity of adipose tissue subtypes and highlighted developmental, functional, and morphological differences within those. Today, adipose tissue in mammals is broadly categorised into white adipose tissue (WAT), brown adipose tissue (BAT), and beige adipose tissue (BeAT).

WAT is a prevalent endocrine organ, involved in the regulation of energy balance via processes of lipolysis, lipogenesis, and energy storage. WAT is predominantly composed of white adipocytes: large, spherical cells that store energy-dense triglycerides (TGs) within a single, unilocular lipid droplet. It's distributed throughout the body with the main depots located in subcutaneous (scWAT) and visceral (vWAT) compartments in both human and rodents (Mandarim-de-Lacerda et al., 2021).

Subcutaneous WAT is the largest depot found beneath the skin; its primary function is safe storage of energy in the form of triacylglycerols (TAGs) and protecting the body from mechanical stress, infection, and heat loss (Vidal and Stanford, 2020). Visceral WAT, is further subdivided into mesenteric, retroperitoneal, and gonadal depots, surrounding vital organs, where it provides insulation and serves as an essential energy source (Bjørndal et al., 2011).

## 1.2 Brown Adipose Tissue

In contrast to its white counterpart, brown adipose tissue, or BAT, has garnered attention for its unique ability to dissipate energy as heat, positioning it as a key player in thermoregulation and metabolic health (Smith, 1964). The evolutionary significance of BAT lies in its early development in mammals, as it has enabled internal heat generation for thermoprotection in endothermic species, especially during reproduction and maternal care (Oelkrug, Polymeropoulos and Jastroch, 2015).

BAT is characterised by its distinct brown coloration, which results from the high mitochondrial content of its multilocular adipocytes. Unlike white adipocytes, which

contain a single large lipid droplet that dominates the cytoplasm, brown adipocytes store energy as TGs within multiple small lipid droplets (Cannon and Nedergaard, 2004; Nedergaard, Bengtsson and Cannon, 2007). Key distinctions between BAT and WAT are demonstrated in Figure 1.

**A.**

| Feature | Brown Adipose Tissue | White Adipose Tissue |
|---|---|---|
| Morphology | 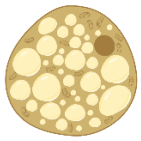 |  |
| Main role | Thermogenesis | Energy storage |
| Cell type | Multilocular | Unilocular |
| Mitochondria | ++++ | low |
| UCP1 marker | ++++ | low |
| Sympathetic innervation | ++++ | + |
| Vascularisation | ++++ | + |

**B.**

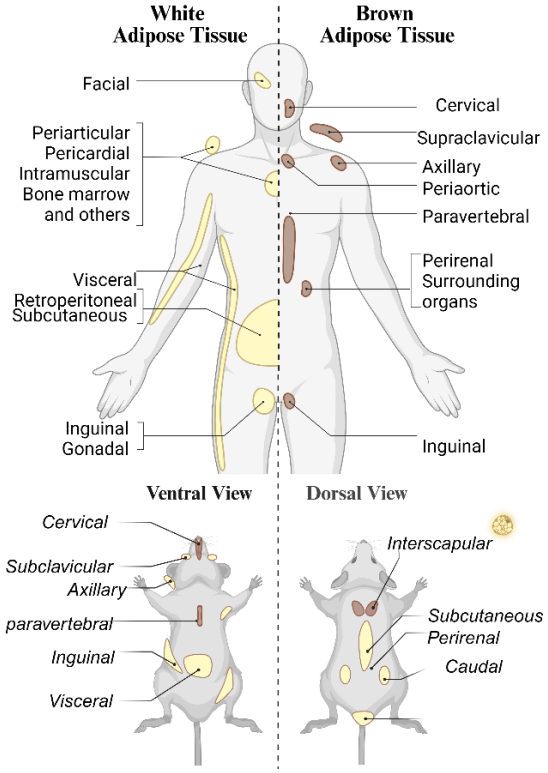


**Figure 1. Summary of adipose tissue characteristics.** Section A provides a summary table outlining the key characteristics and functional properties of each adipose tissue type. Section B illustrates the major white and brown adipose tissue depots observed in humans and in mice.

These specialised brown adipocytes are closely associated with dense vascular networks and are richly innervated by the sympathetic nervous system (SNS) (Bartness, Vaughan and Song, 2010). BAT thermogenic activity is primarily regulated by sympathetic neurons, which release norepinephrine (NE) and neuropeptide Y (NPY) at synapses with brown adipocytes. Consequent NE binding onto β-adrenergic receptors (βAR) activates intracellular pathways within the brown adipocytes, driving non-shivering thermogenesis (Figure 2.). βARs are the G protein-coupled receptors which bind NE and epinephrine (Epi) and are categorized into 3 types: $\beta_1$AR, $\beta_2$AR and $\beta_3$AR (Grogan et al., 2022). While mouse thermogenesis is driven by $\beta_3$AR, more recent findings demonstrated that $\beta_2$AR is

the predominant subtype in humans (Blondin et al., 2020). Close anatomical and functional integration of BAT with sympathetic postganglionic fibers allows for rapid activation and efficient heat production (Carpentier et al., 2018). Overall, the unique morphology of BAT supports its ability to rapidly and effectively mobilise energy for heat production (Himms-Hagen, 1984).

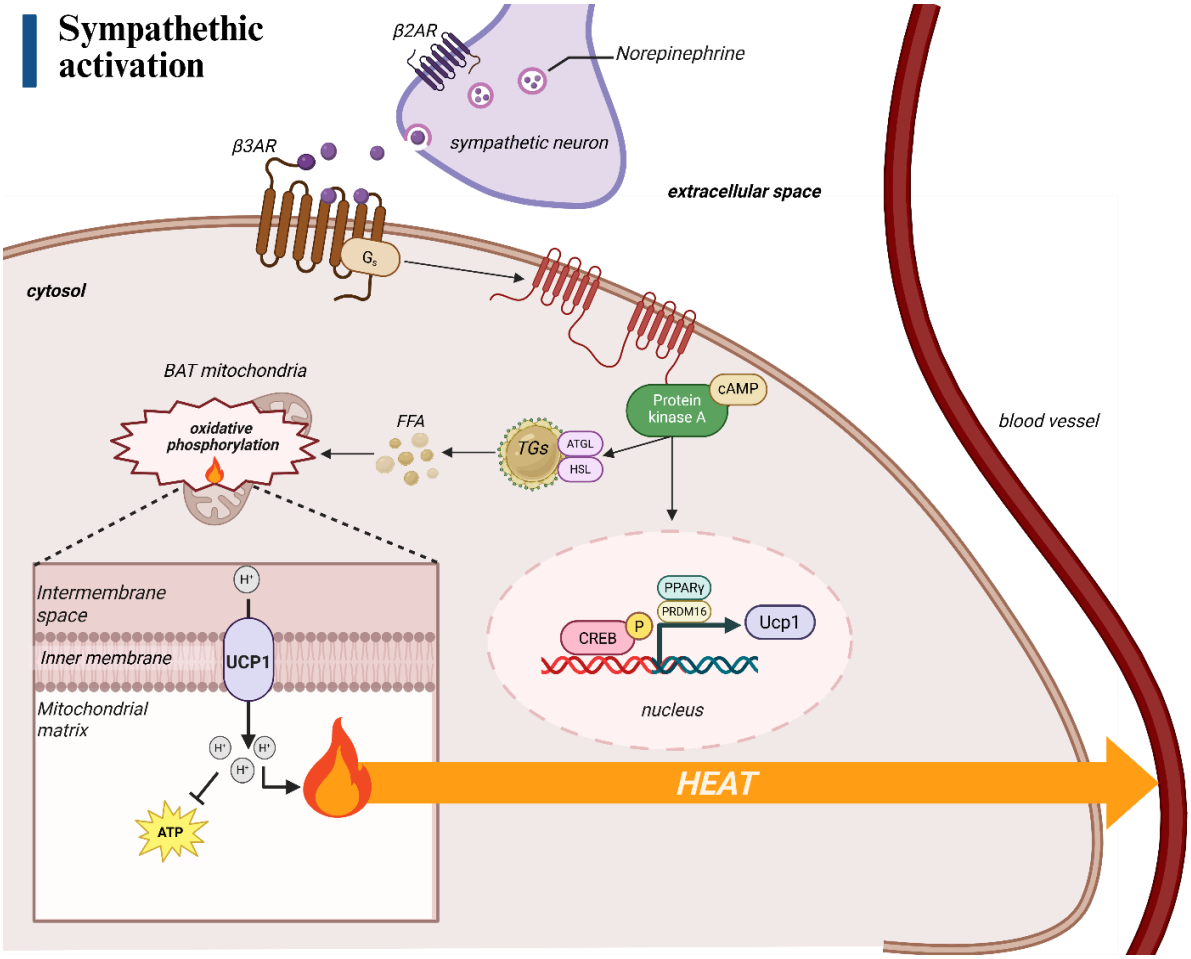


**Figure 2. Detailed sympathetic activation of UCP1-driven non-shivering thermogenesis.**

Cold exposure activates the sympathetic nervous system, where $\beta_2$ARs on sympathetic neurons facilitate NE release. NE binds to β-adrenergic receptors on brown adipocytes, activating the Gs-adenylyl cyclase pathway and elevating intracellular cAMP. This activates protein kinase A (PKA), which phosphorylates adipose triglyceride lipase (ATGL) and hormone-sensitive lipase (HSL), driving triglyceride (TG) hydrolysis and release of free fatty acids (FFAs). FFAs both stimulate uncoupling protein 1 (UCP1) in the mitochondrial inner membrane and provide substrates for β-oxidation. In parallel, PKA phosphorylates cAMP response element-binding protein (CREB), peroxisome-proliferator-activated receptor γ (PPARγ), positive regulatory domain-containing protein (PRDM16) among other regulators - enhancing *Ucp1* transcription. UCP1 activation promotes proton leak across the inner mitochondrial membrane, uncoupling oxidative phosphorylation and dissipating the proton gradient as heat rather than ATP. Together, presynaptic

$\beta_2$AR-driven NE release and βAR-mediated adipocyte signaling sustain non-shivering thermogenesis and adaptive heat production. Figure created with BioRender (https://biorender.com/).

BAT is the most metabolically active peripheral organ in terms of glucose uptake per gram, surpassed only by the brain (Orava et al., 2011). It has been estimated that as little as 50g of fully activated BAT accounts for at least 20% of overall daily energy consumption in an adult human (Rothwell and Stock, 1979). This adaptation not only compensates for excessive heat loss but also protects against obesity and related co-morbidities by increasing energy expenditure and promoting a healthy metabolic profile (Guerra et al., 1998).

## 1.3 Non-shivering thermogenesis (NST)

Thermogenesis is a physiological process by which endothermic mammals produce heat and sustain thermal balance when exposed to colder environments (Ouellet et al., 2012). This thermoregulation is achieved through various mechanisms, such as vasoconstriction of cutaneous blood vessels and skeletal muscle shivering to generate heat (Hertzman, 1959; Mota-Rodas et al., 2021). In addition to shivering, mammals possess autonomically controlled mechanisms of non-shivering thermogenesis (NST) (Nicholls and Locke, 1984; Himms-Hagen, 1984).

NST primarily occurs in brown adipose tissue, a specialised site of adaptive heat production. This unique thermogenic capacity of BAT relies on the function of mitochondrial uncoupling protein 1 (UCP1), also known as *thermogenin* (Palou et al., 1998). UCP1 activation is primarily triggered by cold exposure and governed by the hypothalamus (Arch, 2011). Noteworthy, among the UCP protein family, UCP1 is the only member exclusively expressed in brown adipose fat and directly associated with adaptive thermogenesis (Ricquier, 2011).

Physiologically, the process of thermogenesis can be triggered by various physiological stimuli, such as cold exposure and food intake (diet-induced thermogenesis), which are

centrally integrated by the hypothalamus and brainstem circuits to drive sympathetic outflow (Cannon and Nedergaard, 2004; Nedergaard and Cannon, 2013). Naturally, cold exposure is the most well-defined activator of NST (van der Lans et al., 2014). Upon cold stress, thermal signals are detected by transient receptor potential (TRP) channels located on peripheral sensory neurons (Saito, 2013). These signals are relayed to the central nervous system resulting in heightened sympathetic nervous activity (SNA). At effector level, postganglionic efferent fibers release NE, which binds predominantly to β-adrenergic receptors expressed on brown adipocytes, initiating a cascade of intracellular processes in BAT mitochondria (Okamatsu-Ogura et al., 2020). This interaction initiates the Gs-adenylyl cyclase-cAMP-PKA signaling cascade, which phosphorylates hormone-sensitive lipase to mobilize fatty acids and induces transcriptional programs, culminating in the upregulation of *Ucp1* expression in mitochondria (Murano et al., 2009).

Normally, in mitochondria, the electron transport chain (ETC) pumps protons ($H^+$) from the mitochondrial matrix to the intermembrane space, creating a proton motive force gradient. This electrochemical gradient is used by ATP synthase to drive ATP production. UCP1 function leads to uncoupling of this proton gradient from ATP synthesis. Instead of allowing protons to re-enter the matrix through ATP synthase, UCP1 provides an alternative pathway for proton re-entry, dissipating the gradient as heat rather than storing it as chemical energy (Fedorenko, Lishko and Kirichok, 2012). This heat is then distributed via the bloodstream to help sustain adequate body temperature (Cannon and Nedergaard, 2004; Ricquier, 2011).

Interestingly, UCP1-deficient mice exhibit impaired thermoregulation, as demonstrated by reduced oxygen consumption following $\beta_3$-adrenergic stimulation and pronounced cold sensitivity (Saito, 2013). In the absence of UCP1, the abundance of components of the mitochondrial respiratory chain in BAT is significantly reduced in UCP1-knockout (KO) animals compared to wild-type counterparts (Kazak et al., 2017).

While UCP1 KO rats also display cold sensitivity, the phenotype is less pronounced but still clear (Enerbäck et al., 1997). Despite evidence for a certain degree and capacity for UCP1-independent alternative thermogenic mechanisms, UCP1 remains the defining molecular hallmark of classical NST in thermogenic adipose tissues (Cannon and Nedergaard, 2004).

## 1.4 Anatomical locations and functional relevance of BAT

In rodents and human infants, interscapular BAT, iBAT, is the predominant site of thermogenesis (Lockie et al., 2013; Oelkrug, Polymeropoulos and Jastroch, 2015). Interscapular BAT has been the focus of numerous foundational studies due to its relatively large size, uniform brown adipocyte composition, and accessibility for surgical or imaging analysis (Lockie et al., 2013). Beyond its experimental convenience, iBAT is located between the shoulder blades and is considered functionally relevant due to its anatomical connection to Sulzer's vein, which enables the rapid transport of warmed blood directly to the heart, underscoring its physiological role in systemic thermoregulation (Oelkrug, Polymeropoulos and Jastroch, 2015).

This anatomical positioning of iBAT plays a critical role in protecting small mammals and human neonates from hypothermia, as they rely heavily on BAT-driven thermogenesis, particularly due to their limited skeletal muscle mass and underdeveloped shivering capacity (Oelkrug, Polymeropoulos and Jastroch, 2015; Lidell, 2018). In humans, the iBAT regresses with age, becoming undetectable closer to second decade of life, which long supported the belief BAT-mediated thermogenesis is fully absent in humans (Gilsanz, Hu and Kajimura, 2013). Recent evidence from 18F-flourodeoxyglucose positron emission tomography-computed tomography (FDG PET/CT) imaging, radiological and histological studies disproved this view, revealing the presence of alternative active BAT depots in adult humans (Nedergaard, Bengtsson and Cannon, 2007; Saito et al., 2009; Leitner et al., 2017).

A series of autopsy studies conducted by Heaton et al. provided an insight into the anatomical distribution of BAT in adult humans. In infants BAT is vastly concentrated in the interscapular region, while adults show more diffuse distribution of BAT throughout the body, with active depots commonly found in the supraclavicular, cervical, axillary, paravertebral, mediastinal, and perirenal regions (Heaton, 1972). The supraclavicular depot, located above the clavicle, is the most well-studied BAT site in adults and lies adjacent to the subclavian and carotid arteries, facilitating efficient heat transfer into systemic circulation (Cypess et al., 2009; van Marken Lichtenbelt et al., 2009; Virtanen et al., 2009).

The location of BAT confers an evolutionary advantage by facilitating rapid and targeted heat delivery to vital organs and the central nervous system, enhancing survival during cold stress (Sacks and Symonds, 2013; Oelkrug, Polymeropoulos and Jastroch, 2015).

Considering the biological need for rapid organ warming during acute cold exposure, it is plausible that BAT is strategically distributed around blood vessels to ensure efficient delivery of heat directly to the heart and lungs, while also preventing the return of cooled venous blood from the periphery to the myocardium (Smith, 1964; Sacks and Symonds, 2013).

Importantly, studies show that BAT perfusion more than doubled during acute cold exposure, rising from 7.5 to 15.9 ml per 100 g of tissue per minute (Orava et al., 2011). This is indicative of an increased flow and supply of substrates (such as free fatty acids, glucose and oxygen) for mitochondrial UCP1-dependent oxidative uncoupling and further release of energy in the form of heat into the systemic circulation. In comparison, blood flow in subcutaneous white fat and skeletal muscle showed no significant change, highlighting BAT's unique responsiveness to cold and contribution to maintenance of body temperature homeostasis. Furthermore, BAT perfusion was positively associated with whole-body energy expenditure during cold exposure, unlike other systemic factors such

as thyroid hormones or catecholamines, which showed no such relationship (Sacks and Symonds, 2013).

Given BAT's established role in increasing energy expenditure through NST, targeted activation of these depots represents a promising strategy for obesity management and the treatment of metabolic disorders (Betz and Enerbäck, 2018; Saito et al., 2020; Liu et al., 2023). However, the therapeutic manipulation of BAT requires a nuanced understanding of depot-specific characteristics, including their anatomical location, innervation, vascularisation, and transcriptional patterns.

## 1.5 Sympathetic activation of BAT

The sympathetic nervous system (SNS) is the principal regulator of BAT thermogenesis. Classic and contemporary studies have demonstrated that BAT receives dense sympathetic innervation, essential for initiating heat production in response to cold exposure (Maickel et al., 1967; Bartness et al., 2010).

Morrison et al. have proposed a detailed thermoregulatory network that controls BAT thermogenesis, integrating both afferent sensory input and efferent sympathetic output. The network begins with afferent signals from cutaneous thermal receptors: cool- and warm-sensitive receptors in the skin detect environmental temperature changes and transmit information via dorsal root ganglia (DRG) to second-order neurons in the dorsal horn (DH) of the spinal cord. Cool-sensitive DH neurons activate glutamatergic neurons in the external lateral parabrachial nucleus (LPBel), while warm-sensitive DH neurons project to the dorsal parabrachial nucleus (LPBd). These inputs converge in the preoptic area (POA) of the hypothalamus, where GABAergic interneurons in the median preoptic nucleus (MnPO) inhibit warm-sensitive (W-S) neurons in the medial preoptic area (MPO) in response to cooling, whereas glutamatergic MnPO interneurons excite MPO W-S neurons in response to

warmth. Prostaglandin E2 (PGE2) signaling via EP3 receptors further inhibits MPO W-S neurons during febrile or inflammatory responses.

The MPO W-S neurons then regulate efferent sympathetic outflow to BAT by modulating the activity of downstream sympathoexcitatory neurons in the dorsomedial hypothalamus (DMH). Under cool conditions, inhibition of MPO W-S neurons is relieved, allowing DMH neurons to become active and stimulate BAT premotor neurons in the rostral raphe pallidus (rRPa). These premotor neurons release glutamate and serotonin, which excite sympathetic preganglionic neurons located in the intermediolateral nucleus (IML) of the thoracic spinal cord. These preganglionic neurons, in turn, project via the sympathetic chain to postganglionic neurons that innervate BAT, releasing norepinephrine at the neuro-adipose junction to drive thermogenesis through β3-adrenergic receptor-mediated mechanisms in brown adipocytes (Nakamura & Morrison, 2008).

Additional modulatory inputs refine this efferent output. Excitatory orexinergic neurons from the perifornical lateral hypothalamus (PeF-LH) enhance DMH and rRPa activity, promoting BAT thermogenesis, whereas inhibitory paraventricular hypothalamic (PVH) neurons suppress sympathetic drive under specific physiological conditions. Further fine-tuning occurs via inhibitory projections from the ventrolateral medulla (VLM) and the nucleus of the solitary tract (NTS), which integrate visceral sensory feedback and cardiovascular information, thereby adjusting sympathetic outflow to maintain homeostasis. Together, this hierarchical network ensures that afferent thermal signals from the skin are integrated in the hypothalamus and brainstem, and that efferent sympathetic pathways are precisely modulated to control BAT thermogenesis, balancing energy expenditure with the thermal and metabolic needs of the organism.

Tracing experiments using tyrosine hydroxylase (TH) reporter mice have visualized this innervation in detail, revealing numerous TH-positive fibers intimately associated with brown adipocytes (Murano et al., 2009). Beyond acute activation, SNS stimulation also enhances the

thermogenic capacity of BAT by increasing the number of brown adipocytes, mitochondrial biogenesis, and the expression of *Ucp1* gene (Cannon and Nedergaard, 2004; Nedergaard and Cannon, 2013).

In addition, β-adrenergic signaling is also involved in the browning of WAT, the process by which white adipocytes acquire brown fat-like characteristics, increasing expression of thermogenic genes such as *Ucp1* (Seale et al., 2011). This essentially helps to enhance thermogenic heat-generating capacity under critical environmental conditions. This phenomenon, inducible by cold or pharmacological β-agonism, has become a major focus in obesity and metabolic disease research due to its therapeutic potential (Mottillo et al., 2014; López et al., 2015; González-García et al., 2019). Thus, SNS regulation of BAT thermogenesis represents both a rapid response mechanism to thermal stress and a long-term adaptive system with significant implications for metabolic homeostasis and energy expenditure.

These sensory circuits likely play a role in a feedback loop that fine-tunes sympathetic nervous output based on the current state of BAT activity and thermogenic demand. Studies have shown that sensory denervation of BAT impairs thermogenic capacity of the tissue, highlighting importance of the bidirectional communication between BAT and SNS (Díaz-Castro, Morselli and Claret, 2024).

### 1.5.1 Pharmacological activation of BAT

Cold exposure is the primary natural trigger of brown adipose tissue thermogenesis, however pharmacological approaches, such as adrenergic receptor agonists, thyroid hormone analogs, and emerging sympathofacilitators offer alternative strategies to stimulate BAT activity (Carpentier et al., 2022; Mahú et al., 2020).

While induction of BAT-thermogenesis is a compelling strategy for increasing energy expenditure and promoting weight loss, pharmacological activation of BAT raises important

safety concerns. Most proposed BAT-activating strategies rely on enhancing sympathetic nervous system outflow and stimulating β-adrenergic receptor-mediated thermogenesis. However, systemic activation of β-adrenergic signalling lacks tissue specificity and has been consistently associated with adverse cardiovascular effects, including tachycardia, hypertension, and an increased risk of myocardial infarction or stroke (Singh et al., 2021; Straat et al., 2023). These effects are thought to arise from off-target activation of β-adrenergic receptors expressed on cardiomyocytes and vascular smooth muscle cells, resulting in increased cardiac workload and haemodynamic stress (Straat et al., 2023).

These concerns are further underscored by clinical experience with sympathomimetic weight-loss drugs. Early anti-obesity agents, including amphetamine-like sympathomimetics, increased energy expenditure through broad stimulation of the sympathetic nervous system but were ultimately withdrawn due to serious cardiovascular complications, such as pulmonary hypertension and valvular heart disease (Bersoux et al., 2017). Importantly, increased thermogenic drive itself may further exaggerate cardiovascular strain, as elevations in energy expenditure are accompanied by increased oxygen demand and cardiac output, leading to rises in heart rate even in the absence of overt cardiac receptor targeting (Singh et al., 2021).

Collectively, these observations highlight a key limitation of systemic BAT activation strategies and emphasize the need for approaches that enhance thermogenesis while minimizing non-selective sympathetic stimulation and cardiovascular risk. As such, strategies aimed at enhancing BAT activity, particularly through sustained sympathetic stimulation, should carefully consider systemic cardiovascular effects rather than assuming depot-specific metabolic benefits in isolation (Straat et al., 2023). Interestingly, recent efforts have focused on mitigating these cardiovascular risks by developing sympathofacilitators that selectively enhance BAT-directed sympathetic activity without engaging central or cardiac adrenergic receptors (Mahú et al., 2020). For example, PEGylated amphetamine (PEGyAMPH) cannot

enter the brain but stimulates peripheral sympathetic neurons via $\beta_2$-adrenoceptors, promoting lipolysis and BAT thermogenesis in mice while avoiding changes in heart rate, food intake, or locomotor activity (Mahú et al., 2020).

Collectively, while BAT activation remains a promising therapeutic avenue for obesity and metabolic disease, these findings underscore the need for careful evaluation of safety, receptor specificity, and physiological context to avoid unintended adverse outcomes. Importantly, BAT is not a homogeneous tissue; rather, it consists of anatomically and functionally distinct depots that differ in developmental origin, cellular composition, vascularization, innervation, and responsiveness to sympathetic and hormonal cues (Sidossis and Kajimura, 2015; Lynes and Tseng, 2018). This heterogeneity introduces an opportunity for more refined therapeutic strategies, whereby selectively targeting specific BAT depots or regulatory pathways may enhance thermogenic output while limiting systemic sympathetic activation and cardiovascular risk. Understanding depot-specific differences in thermogenic capacity, neural control, and molecular signature is therefore critical for developing safer, more precise BAT-based interventions.

## 1.6 Thermogenic Capacity and Functional Heterogeneity of BAT

Numerous studies have highlighted the anatomical and functional versatility of BAT across different regions of the human body (Sidossis and Kajimura, 2015; Lynes and Tseng, 2018). This regional heterogeneity is not only evident in the anatomical distribution of BAT depots, but also reflected in their distinct gene expression profiles, thermogenic capacities, and responsiveness to various physiological stimuli (Duerre and Galmozzi, 2022). Such diversity suggests that different depots may contribute uniquely to systemic energy expenditure and metabolic regulation. Importantly, several groups have now reported that the brown adipocytes (even within the same anatomic depot, and particularly in the different depots)

may have heterogeneous *Ucp1* expression, as well as expression of other thermoregulatory genes (Spaethling et al., 2015).

Study by Song et al. (2019) used single-cell RNA sequencing to identify two different populations of brown adipocytes: high thermogenic brown adipocyte (BA-H) and low thermogenic brown adipocyte (BA-L). These subtypes differed in expression of classic thermogenic markers (e.g., UCP1, $\beta_3$-AR) and genes involved in oxidative phosphorylation, β3-adrenergic signaling, lipolysis, glycolysis, fatty acid oxidation, and the TCA cycle.

Overall, these findings indicate that brown adipocytes are functionally heterogeneous, with a distinct subpopulation specialized for robust thermogenesis that can be defined by its unique metabolic and gene expression profiles. This heterogeneity likely reflects the mixed cellular composition of BAT depots, which contain brown, beige, and white adipocytes, as well as potentially other, yet uncharacterized, adipose cell types.

With BAT-specific signature genes now identified, the key next step will be to investigate early differentiation pathways and to characterize the molecular and transcriptional profiles of less-studied BAT depots. This will not only deepen our understanding of depot-specific thermogenic capacity but also inform the development of targeted therapies for obesity and related metabolic disorders (Xue et al., 2015).

## 1.7 Adipocyte Lineage Commitment and Differentiation

Adipocyte differentiation occurs in two major phases: (1) commitment of multipotent mesenchymal stem cells to the pre-adipocyte lineage, and (2) terminal differentiation of pre-adipocytes into mature adipocytes. These developmental stages are tightly regulated by lineage-specific transcription factors and epigenetic modifications, including histone modifications and changes in chromatin structure. These coordinated changes establish unique chromatin landscapes that enable proper adipogenic progression (Nic-Can et al., 2019).

Comprehensive *in vitro* and *in vivo* studies have helped identify key regulators of this process. Insights into WAT adipogenesis come from studies on clonal pre-adipocyte cell lines, such as 3T3-L1 and 3T3-F442A, which differentiate into mature adipocytes in response to hormonal cues (Rosen and Spiegelman, 2000; Gesta et al., 2007). Differentiation in these models typically proceeds through growth arrest, clonal expansion, and stages of early and terminal differentiation. Notably, adipocyte development often occurs in spatial clusters, possibly facilitated by paracrine signals from nearby mature adipocytes.

### 1.7.1 Lineage Origins: BAT *versus* WAT

Although both white and brown adipose tissue originate from mesenchymal stem cells, they commit to distinct developmental lineages early in development (Figure 3). Brown preadipocytes arise from Myf5-positive progenitors, a lineage also shared with skeletal muscle and display gene expression profile closely resembling that of myogenic cells. In contrast, white adipocytes originate from Myf5-negative progenitors (Figure 3) , reflecting a separate developmental path. It's believed that while white adipocyte progenitors derive from the stromal-vascular fraction (SVF) of adipose tissue, interscapular brown adipose tissue resides in the central dermomyotome, a region that also gives rise to skeletal muscle (Birerdinc et al., 2013; Sanchez-Gurmaches and Guertin, 2014).

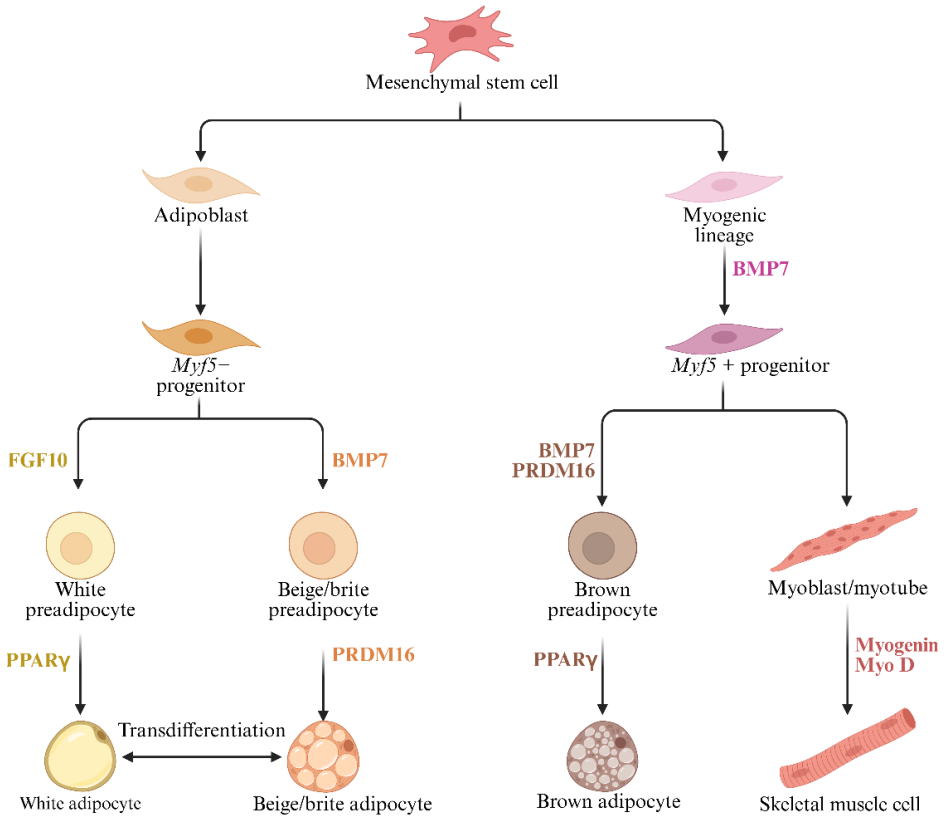


**Figure 3. Detailed scheme of developmental origins and differentiation pathways of adipocytes.** Mesenchymal stem cells give rise to distinct adipocyte types, depending on specific signaling cues. White adipocytes arise from FGF10-responsive precursors through PPARγ activation, leading to the formation of unilocular cells specialized in lipid storage. Brown adipocytes originate from $Myf5^{+}$ progenitor cells, which also give rise to skeletal muscle. Their commitment to the brown adipocyte lineage is orchestrated by bone morphogenetic protein 7 (BMP7) and the transcriptional regulator PRDM16. Beige adipocytes, on the other hand, develop within white adipose depots from $Myf5^{-}$ precursors under the influence of BMP7 and PRDM16. These beige cells can acquire thermogenic brown fat-like properties and may revert to white adipocytes in response to environmental or hormonal factors. Myogenic transcription factors such as Myogenin and MyoD direct differentiation toward the muscle lineage from the same progenitor pool.

BAT develops earlier during embryogenesis, reaching its highest proportion relative to body weight at birth coinciding with the high thermogenic demand in neonates, and gradually declines with age in both humans and rodents. Conversely, WAT forms later (mid-gestation in humans and postnatally in rodents) and continues to expand throughout life to accommodate body's energy storage needs (Symonds, Pope and Budge, 2015).

As briefly mentioned previously, white adipose tissue can transition into brown adipocyte phenotype, a process known as "browning" of WAT. Under specific stimuli such as cold

exposure or $\beta_3$-adrenergic receptor activation, white adipocytes can acquire characteristic properties of brown adipocytes to increase the number of thermogenic brown-like cells. These are also known as “beige” or “brite” fat cells. Importantly, these beige cells do not originate from Myf5-expressing progenitors, distinguishing them from classical brown adipocytes, and supporting the existence of at least two distinct thermogenic adipocyte lineages (Seale, 2007). Although the precise identity of these beige progenitors remains unclear, current evidence suggests that they belong to a distinct population of inducible thermogenic precursors residing within WAT (Wu et al., 2012).

## 1.8 Molecular and Transcriptional Control of BAT

The recruitment and activation of brown adipocytes is primarily mediated by β-adrenergic signaling, which upregulates numerous thermogenic genes - most notably *Ucp1* (Fedorenko, Lishko and Kirichok, 2012).

The establishment of adipocyte identity is orchestrated by a tightly regulated network of transcription factors (Kajimura, Seale and Spiegelman, 2010). These DNA-binding proteins modulate RNA polymerase II activity to either activate or repress gene transcription by binding to specific motifs in promoter regions and distal regulatory elements such as enhancers and silencers (Kolovos et al., 2012). Despite their differing developmental origins, brown and white adipocytes share a core transcriptional program that drives adipocyte differentiation.

Studies using inducible preadipocyte cell lines have revealed that a key molecular switch for both brown and white adipocytes is regulated by the transcription factors peroxisome proliferator-activated receptor γ (PPARγ) and members of the CCAAT/enhancer-binding protein (C/EBP) family, including C/EBPβ, C/EBPδ, and C/EBPα (Lefterova et al., 2008; Lee et al., 2019). Early in adipogenesis, C/EBPβ and C/EBPδ are transiently upregulated, initiating the expression of PPARγ and C/EBPα. PPARγ acts as the master regulator of adipogenesis,

while C/EBPα supports PPARγ expression and synergistically enhances the expression of key adipocyte genes. Importantly, while this transcriptional cascade can induce white adipocyte differentiation in mesenchymal cells, it is insufficient to drive brown adipocyte identity (Park, 2014). For the scope of this thesis, emphasis is placed on several key BAT-associated genes and transcriptional regulators.

**PPARγ (peroxisome proliferator-activated receptor gamma)**

PPARγ is a member of the nuclear hormone receptor superfamily, which drives the adipogenesis of both brown and white adipose tissue (Tontonoz et al. 1994; Barak et al. 1999; Rosen et al. 1999; Nedergaard et al. 2005). The critical role of PPARγ in humans is highlighted by its involvement in familial partial lipodystrophy type 3 (FPLD3), a rare genetic disorder caused by loss-of-function mutations in the *PPARG* gene. Individuals with FPLD3 typically have an abnormal fat distribution which is often accompanied by severe metabolic complications, such as type 2 diabetes. Most FPLD3-associated PPARG mutations are found in either the DNA-binding domain (DBD) or the ligand-binding domain (LBD) leading to broad functional impairments. Extensive research has established that PPARγ is associated with another family of transcription factors - CCAAT/enhancer-binding proteins (C/EBPs), including C/EBPα, C/EBPβ, and C/EBPδ (Kajimura, Seale and Spiegelman, 2010).

At the early stages of adipocyte differentiation, *C/EBPβ* and *C/EBPδ* are transiently upregulated and play essential roles in inducing the expression of *PPARγ* and *C/EBPα*. While PPARγ acts as the primary regulator driving adipocyte differentiation, C/EBPα is necessary for sustaining *PPARγ* expression (Rosen et al., 1999; Rosen et al., 2002; Wu et al., 1999). Moreover, interestingly induction of prolonged high expression of *C/EBPβ* in white adipocytes has been shown to upregulate genes typically associated with brown fat.

More recent research has identified additional transcriptional regulators that either promote or inhibit brown fat cell development (discussed below). Additionally in C/EBPα-ablated mice show that the development of WAT, but not BAT is disrupted (Linhart et al. 2001), suggesting that *PPARγ* expression in WAT is more dependent on C/EBPα than in BAT.

**Pgc-1α (the nuclear PPARγ gamma coactivator)**

Transcriptional coactivator Pgc-1α is central to this thermogenic program, enhancing the activity of transcription factors like PPARγ and thyroid hormone receptor to promote *Ucp1* expression and mitochondrial biogenesis (Wu, Cohen and Spiegelman, 2013).

Overexpression of *Pgc-1α* in white preadipocytes can induce brown fat-like thermogenic gene expression. While brown adipocytes lacking Pgc-1α can still differentiate, they show impaired induction of thermogenic genes, underscoring Pgc-1α's functional, rather than developmental importance. Several factors regulate Pgc-1α at both transcriptional and post-translational levels. Positive regulators include FOXC2, CREB, SIRT3, SRC-1, nitric oxide, and p38 MAP kinase, while repressors like RIP140, necdin, and SHP inhibit its expression or activity. 4E-BP1 acts at the translational level to suppress Pgc-1α protein synthesis, while p38 MAP kinase can phosphorylate Pgc-1α to enhance its function (Othman Abu Shelbayeh et al., 2023). Its interaction with transcription factors such as PPARγ, PPARδ, and NRF-1 allows for recruitment of nuclear coactivators like CBP/p300, driving robust transcription of thermogenic genes (Cheng, Ku and Lin, 2018).

**PRDM16 (PRD1-BF-1-RIZ1 homologous domain-containing protein-16)**

PRDM16, a zinc finger-containing protein with a PR (PRD1-BF1-RIZ1 homologous) domain, a major transcriptional activator of BAT-selective gene program, expressed selectively in BAT; when overexpressed in white adipocyte precursors, PRDM16 drives differentiation into brown fat-like phenotype both *in vitro* and *in vivo*, while simultaneously repressing WAT-associated genes (Seale et al., 2007; Kajimura et al. 2008). Specifically,

PRDM16 induces activation of thermogenic genes (*Ucp1*, *Pgc-1α*, and *D2*) and BAT-selective genes (*Cidea* and *Elovl3*), along with other mitochondrial genes (Seale et al. 2007, 2008; Kajimura et al. 2008).

These effects are mediated at least in part through interactions with transcriptional co-regulators Pgc-1α and Pgc-1β, independent of direct DNA binding.

Furthermore, PRDM16 can direct a bidirectional switch in cell fate between skeletal myoblasts and brown fat cells. Lineage tracing studies support this by demonstrating that BAT, but not WAT, derives from Myf5-expressing precursors, a lineage shared with skeletal muscle, highlighting a developmental link between muscle and brown adipose tissue. Ablation of PRDM16 showed nearly total loss of the brown fat characteristics *in vitro* (Seale et al. 2007). Interestingly PRDM16 deletion from BAT precursor promotes differentiation into skeletal muscle-like phenotype. Consistent with this, BAT from PRDM16 ablated mice exhibits an abnormal morphology with dramatically reduced expression of thermogenic genes and elevated expression of muscle-specific genes at embryonic day 17 (Seale et al. 2008). This evidence positions PRDM16 as a critical driver of brown adipocyte differentiation.

**CIDEA (Cell death-inducing DNA fragmentation factor-like effector A)**

CIDEA, a member of the CIDE protein family, plays a pivotal role in the regulation of thermogenesis and adipocyte browning through transcriptional control of UCP1. It is considered a BAT-specific marker gene, as its mRNA expression is enriched in brown adipose tissue (at least 50-fold higher compared to other tissues). Mechanistically, CIDEA interacts with UCP1 and inhibits its uncoupling activity, thereby establishing a higher activation threshold for thermogenesis.

In the absence of *Cidea* expression, UCP1-mediated thermogenesis is enhanced, leading to elevated energy expenditure and reduced fat accumulation. Notably, high *Ucp1* expression precedes the induction of BAT-specific genes during the browning process, suggesting that

the release of CIDEA-mediated repression on *Ucp1* may serve as a molecular switch initiating the full conversion of white adipocytes into thermogenic beige cells.
By modulating the threshold and extent of UCP1 activation, CIDEA functions as a gatekeeper of adaptive thermogenesis, energy expenditure, and fat storage (Jash et al., 2019).

**Elovl3 (elongation of very long-chain fatty acids 3)**

Elovl3, originally identified as Cig30, is a member of the Elovl family of fatty acid elongases, though the molecular basis of its substrate specificity remains unclear. It catalyzes the elongation of fatty acids up to 24 carbons and is most prominently expressed in BAT, with additional expression in the liver, skin, kidney, white adipose tissue, and heart. *Elovl3* expression is strongly induced during BAT activation, particularly in response to chronic NE stimulation, high-calorie diet, and early postnatal development. Functional studies in Elovl3 KO mice revealed impaired BAT recruitment during acute cold exposure, accompanied by deficits in skin barrier integrity. Although knockout mice could ultimately survive prolonged cold, they relied predominantly on skeletal muscle shivering rather than BAT thermogenesis. Moreover, in warm-acclimated KO mice, BAT exhibited reduced lipid storage and diminished metabolic activity upon NE stimulation. Collectively, these findings suggest that Elovl3 is essential for lipid accumulation and metabolic activation of BAT during the early recruitment phase but is not strictly required for long-term cold adaptation (Westerberg et al., 2006).

## 1.9 Introduction to paravertebral brown adipose tissue (pBAT)

Paravertebral brown adipose tissue (pBAT) is a depot positioned in thoracic paravertebral space and consistently found in both humans and rodents. Numerous studies have previously reported that human pBAT exhibits metabolic activity with increased glucose uptake upon cold exposure, visualized with both 18F-FDG PET and SPECT/CT imaging with the mitochondrial tracer 99mTc-methoxyisobutylisonitrile (99mTc-MIBI) (Goetz et al.).

Despite extensive research into human BAT, most attention has focused on supraclavicular depot, scBAT, while the paravertebral BAT depot remains largely unexplored. For a while, supraclavicular BAT was considered the human equivalent of the interscapular BAT depot in small mammals. However, this assumption has been challenged by more recent findings, that unlike interscapular depot in mice the supraclavicular region is made of beige, brown and white adipocytes. The constitutive interscapular BAT depot, classic site of thermogenesis in rodents, is mostly homogeneous, composed almost of thermogenic brown adipocytes. In contrast, scBAT is highly infiltrated with white/beige adipocytes, which could potentially mean lower thermogenic capacity of this depot (Lidell et al., 2013). Additionally, as a superficial depot, scBAT is also more susceptible to age and obesity related whitening (Von Bank et al., 2021).

Current research is focused on identifying alternative BAT depots and determining whether these depots function as the human equivalent of interscapular BAT.

Paravertebral BAT has captured our interest due to several factors:

1) Our preliminary results show that pBAT is engulfed in sympathetic ganglia, with the left T3 ganglion being surrounded by adipose tissue immunostained for TH and UCP1 (as shown on Figure 4). The dense sympathetic innervation and positive UCP1 staining strongly suggests sympathetic input into the tissue and that adipose tissue surrounding sympathetic ganglia is thermogenic. Given that classical thermogenic BAT function relies on intricate network of sympathetic and vascular innervation, we believe this positioning could have an implication on pBAT's thermal and metabolic function.

2) Evidence from small mammals and hibernating species suggests that BAT located adjacent to the spinal cord and sympathetic chain plays a critical role in thermoprotection of neural structures during cold exposure. pBAT is anatomically positioned in the paraspinal space, adjacent to vital organs, major vessels, and the sympathetic chain. It is plausible that this

location could be an evolutionary strategy to enable countercurrent heat exchange and allow local warming of the thoracic spinal cord and sympathetic ganglia, thereby maintaining thermoregulatory autonomic outflow and supporting prolonged BAT activation. In rodents, BAT is positioned in a way that heat generated during cold exposure can be transferred via countercurrent vascular mechanisms to vital thoracic organs, the spinal cord, and the sympathetic chain (Smith, 1964). In humans, paravertebral BAT may similarly contribute to warming the thoracic spinal cord and sympathetic ganglia, either directly or indirectly through nearby intercostal vessels supplying spinal circulation (Sacks and Symonds, 2013). These features imply that paravertebral and thoracic BAT depots may help preserve neural, autonomic, and neuromuscular function during hypothermia (Sacks and Symonds, 2013).

3) In humans, pBAT may also benefit from vascular connections, such as intercostal arteries branching into spinal vessels and linking with the anterior spinal artery, further facilitating localized heat delivery to neural structures (Sacks and Symonds, 2013).

4) Similarly to the last point, pBAT's location could also be evolutionary adaptation to provide heat to major organs in the thoracic cavity, such as heart and major arteries.

5) Additionally, evidence from animal studies indicates that deeper depots of BAT are lost later in life compared with superficial depots, suggesting greater resilience to age-associated decline (Ou et al., 2022). Similarly, age-related reductions in Ucp1 expression and BAT mass appear to affect more superficial depots first, while some deeper depots retain activity for longer (Yu et al., 2024). Indeed, there is sufficient evidence of pBAT persisting into adulthood in humans, unlike classical iBAT.

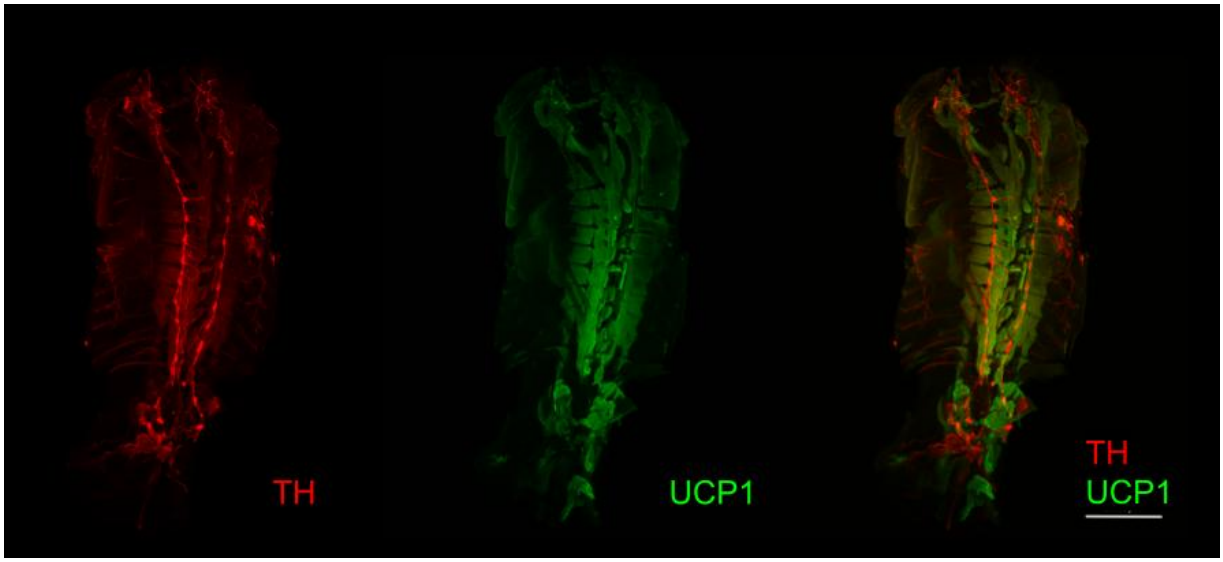


**Figure 4. Representative immunofluorescence images showing TH and UCP1 signal distribution.** Representative images of tissue stained for tyrosine hydroxylase (TH, red) and uncoupling protein 1 (UCP1, green). Individual channels are shown separately (left: TH; middle: UCP1), alongside a merged image (right). Areas of apparent signal overlap are visible in the merged panel. Images are presented for qualitative visualization of marker localization and suggest sympathetic innervation of pBAT.

The above-discussed factors indicate that paravertebral BAT could be part of a highly integrated neural-metabolic axis that enables rapid thermogenic responses. However, such a role has not been described or characterised, representing a significant gap in our understanding of BAT's functional diversity.

Investigating pBAT could therefore provide valuable insights into the mechanisms that maintain functional BAT in humans, as well as its role in core thermoregulation and neurovascular protection. To address these knowledge gaps, we aimed to characterise the molecular and transcriptional profile of paravertebral BAT and compare it with other well-studied depots.

### 1.9.1 Hypothesis and aims of this research

We hypothesize that the paravertebral BAT (pBAT) depot is a functionally distinct subset of brown adipose tissue that contributes to localized thermogenesis, protecting neural structures and sustaining autonomic output during cold exposure in mammals. This project aims to characterize the transcriptional profile of pBAT and evaluate its thermogenic potential in murine models. A pilot study confirmed the expression of key thermogenic genes in pBAT, validating its functional relevance.

To interrogate the mechanisms driving thermogenesis, we applied two complementary interventions:

1. Acute cold exposure: animals were exposed to 4°C for 24 hours to mimic an environmental cold challenge.

2. Pharmacological activation: administration of the $\beta_2$-adrenergic receptor ($\beta_2$-AR) agonist Clenbuterol.

The rationale for using Clenbuterol stems from recent evidence showing $\beta_2$-AR expression on sympathetic neurons innervating BAT. While the postsynaptic roles of $\beta_2$-ARs in adipocytes are well established, their potential presynaptic function in sympathetic neurons remains poorly defined. Early pharmacological studies in the rat stellate ganglion, which innervates the heart, demonstrated that presynaptic $\beta_2$-AR activation amplifies cAMP-PKA signaling, elevates intracellular $Ca^{2+}$, and facilitates norepinephrine and epinephrine release (Bardsley et al., 2018). These findings suggest that a similar presynaptic $\beta_2$-AR-mediated mechanism may operate in sympathetic neurons innervating BAT.

Building on this hypothesis, our laboratory provides the first direct evidence of $\beta_2$-AR expression in sympathetic neurons of the stellate ganglion that innervate the thermogenic iBAT depot in mice. Activation of these $\beta_2$-ARs exerts sympathofacilitatory effects,

enhancing NE-evoked sympathetic responses in vitro, promoting iBAT thermogenesis, and contributing to maintenance of healthy body weight independently of food intake. Mechanistically, these effects are likely mediated via the cAMP-PKA signaling pathway, which supports sympathetic neuron growth and survival (Cheung et al., 2025).

Importantly, targeting $\beta_2$-ARs at the level of sympathetic ganglia represents an attractive and translationally relevant strategy. Because the stellate ganglion innervates iBAT in mice, selective presynaptic stimulation of $\beta_2$-ARs can be readily tested in well-established murine models, allowing precise mechanistic interrogation of neural control of BAT thermogenesis prior to human translation.

Having established the effects of presynaptic $\beta_2$-AR activation in iBAT, we next investigated whether enhanced sympathetic signaling influences thermogenic gene expression across other adipose depots, with a particular focus on pBAT. Clenbuterol administration in our mouse models allowed us to probe whether presynaptic $\beta_2$-AR stimulation within sympathetic neurons projecting to pBAT modulates the expression of key thermogenic markers.

We examined genes regulating brown adipogenesis (Prdm16), lipid storage and glucose uptake (Cidea, Elovl3), and thermogenic function (Ucp1, Pgc-1α). By comparing gene expression in pBAT with untreated controls and other adipose depots, this study aims to elucidate depot-specific transcriptional and functional responses to cold and adrenergic stimulation and assess whether the gene expression profile of pBAT resembles classical iBAT.

# 2

# Methods

## Contents



## 2.1 Mice handling

**Animals**

Experiments were executed using wild-type (WT) C57BL/6 mice obtained from Charles River Laboratories and housed in the University of Oxford Animal Facility under specific pathogen-free conditions. Environmental parameters were maintained at 21 ± 1°C and 50 ± 10% humidity, with a 12h light/dark cycle. Animals had ad libitum access to standard chow and water, unless otherwise stated. Male mice aged 8-16 weeks were used for metabolic phenotyping, as detailed in the respective figure legends. All experimental procedures complied with the UK Home Office regulations, the University of Oxford institutional guidelines, and the University of Iowa Animal Care and Use Committee protocols.

**Mice Housing at Thermoneutral Temperature and Exposure to Cold Stress**

C57BL/6J male mice at 8-weeks old were housed at thermoneutrality (~30°C) for 7 days to eliminate cold-induced activation of BAT that occurs under standard housing conditions (~21 °C). This prevents baseline sympathetic stimulation of BAT, enabling a clearer assessment of β-adrenergic receptor agonist effects. Moreover, housing at thermoneutrality better reflects human thermal conditions, enhancing the translational relevance of the findings. At this point, the thermoneutrality-only control group was culled, while the remaining mice were exposed to 4 °C for 24 hours, with rectal temperatures measured every 6 hours to ensure core temperature remained above the 30 °C welfare stop-point. Both groups were then anesthetised with pentobarbital (4 mg/g body weight) and transcardially perfused with 20 mL of PBS (1×) containing heparin (20 U/mL), followed by 20 mL of 4% paraformaldehyde (PFA) in PBS (1×). This experimental design minimized confounding thermal stress, ensured animal welfare, and provided well-preserved tissue for downstream analyses.

## 2.2 Immunohistochemistry with tissue clearing (iDISCO)

**Fluorescence-guided dissection and histology**

C57BL/6J male mice were anaesthetized and perfused with 50 mL PBS + heparin 20U/mL, followed by a seconder fusion with 50 mL 4% PFA/PBS to remove excessive blood that could limit visibility during the dissection. Next, BAT samples were fixed in 1x PBS/PFA at 4 °C overnight with shaking for 12-16 hours, then at room temperature for 1 hour. Finally, the samples were washed in PBS while shaking at room temperature for 30 minutes. Last step has been repeated 3 times.

**Immunohistochemistry with tissue clearing (iDISCO)**

We optimised iDISCO+ protocol for whole-body and torso preparations, considering the sample size, lipid content, and the preservation of delicate sympathetic structures. Our

adapted workflow enabled us to maximise antibody penetration and tissue transparency, resulting in high-quality images. Importantly, we found that exposure of the sample to air, and consequent oxidation, leads to reduces tissue transparency and affects the image quality. For this reason, we minimised the air exposure of the samples and ensured that all incubations were performed in filled tubes, with 50 mL Falcon tubes preferred during washes to ensure homogeneous antibody distribution and reduced aggregation.

Torso dissections were designed to preserve the stellate ganglia and sympathetic chain, requiring removal of thoracic viscera while minimising disruption to key innervation sites. We performed laminectomy, a procedure by which part of the posterior region of each vertebra is being removed to expose the spinal cord and allow comprehensive analysis. This was followed by a week-long treatment in 10% EDTA (pH 8-9) for sufficient and effective decalcification without compromising tissue integrity.

**Pretreatment**

Sample pretreatment involved graded methanol dehydration followed by DCM delipidation, which was particularly important for lipid-rich tissues such as adipose depots, brain, and spinal cord. Insufficient delipidation produced incomplete clearing, reinforcing the need for extended solvent washes in these tissues. A bleaching step in methanol/hydrogen peroxide enhanced optical clarity by reducing pigmentation, especially when performed under strong illumination.

**Immunolabeling**

For immunolabeling, prolonged incubations were necessary due to the size and density of the samples. A two-day permeabilization and blocking phase at 37°C optimized antibody access, followed by primary and secondary antibody incubations of at least one week each. Washes between antibody steps were extensive, with multiple buffer changes over 48 h, which prevented antibody trapping and reduced background fluorescence.

**Clearing**

Finally, refractive index matching was achieved through sequential treatment with DBE and ethyl cinnamate (ECi). We observed that filling tubes to the top was especially critical at this stage to prevent oxidation artifacts. Interestingly, leaving samples embedded in ECi for several additional days prior to imaging improved transparency and yielded clearer images, particularly in large tissue blocks.

After tissue clearing, light-sheet fluorescence imaging was carried out to obtain high-resolution three-dimensional visualization of the specimen using UltraMicroscope II. The lengths (μm) determined using the Surface and FilamentTracer tools in Imaris 10.

## 2.3 Treatment

**Exposure to $\beta_2$-AR-agonist Treatment with Clenbuterol**

For selective activation of $\beta_2$-AR, C57BL/6J mice were treated with Clenbuterol in drinking water (30mg/L) for 14 days starting when they were 8 weeks old. Following the treatment, mice were euthanised via $CO_2$ inhalation and perfused with ice-cold PBS for 5 minutes. Following perfusion, tissues were rapidly excised, placed immediately on dry ice, and stored at the appropriate temperature until further processing.

**Isolation of adipose tissues**

Adipose tissue depots, including subcutaneous white adipose tissue, gonadal white adipose tissue, interscapular brown adipose tissue, and paravertebral brown adipose tissue were obtained from both the cold-exposure and Clenbuterol-treated mice.

iBAT was isolated by making an incision along the dorsal midline between the shoulder blades to expose the underlying brown fat depot (identified as the darkly pigmented fat pad located between the scapulae). The iBAT pad was carefully separated from adjacent muscle and connective tissue using fine forceps.

gWAT was dissected by opening the abdominal cavity and gently removing the fat pads surrounding the gonads, ensuring minimal disruption to adjacent organs.
scWAT was harvested from the inguinal region by making a skin incision and lifting the subcutaneous fat layer away from the underlying muscle. All tissues were collected with care to avoid contamination from neighboring tissues and stored at -80°C until further processing.
For the dissection of pBAT, the region adjacent to the vertebral column was carefully exposed under a dissecting microscope. The overlying connective tissues and muscles were gently separated to reveal the brown fat depot located paravertebrally. Using fine forceps, pBAT was dissected free from surrounding structures to avoid contamination with neighboring tissues. This method ensured high-purity isolation of the paravertebral brown adipose tissue for downstream transcriptional analyses. All dissected depots were immediately placed in pre-chilled PBS on ice prior to further processing for transcriptional analyses.

## 2.4 qRT-PCR

**RNA isolation and qRT-PCR**

Frozen adipose tissue samples were homogenized in Trizol reagent using a bead-based homogenizer. Total RNA was extracted following a standard phenol-chloroform protocol with subsequent DNase treatment and ethanol precipitation to ensure purity. RNA quality and concentration were assessed using a Nanodrop spectrophotometer. Two micrograms of total RNA were reverse-transcribed into cDNA using the SuperScript III First-Strand Synthesis System (Invitrogen) according to the manufacturer's instructions. Quantitative real-time PCR (qRT-PCR) was performed using Platinum SYBR Green qPCR SuperMix-UDG (Invitrogen) on a Real-Time PCR Detection System (Bio-Rad). Relative gene expression levels were calculated using the $2^{-\Delta Ct}$ method, normalizing target gene

expression to hypoxanthine phosphoribosyltransferase 1 (HPRT1) housekeeping reference gene.

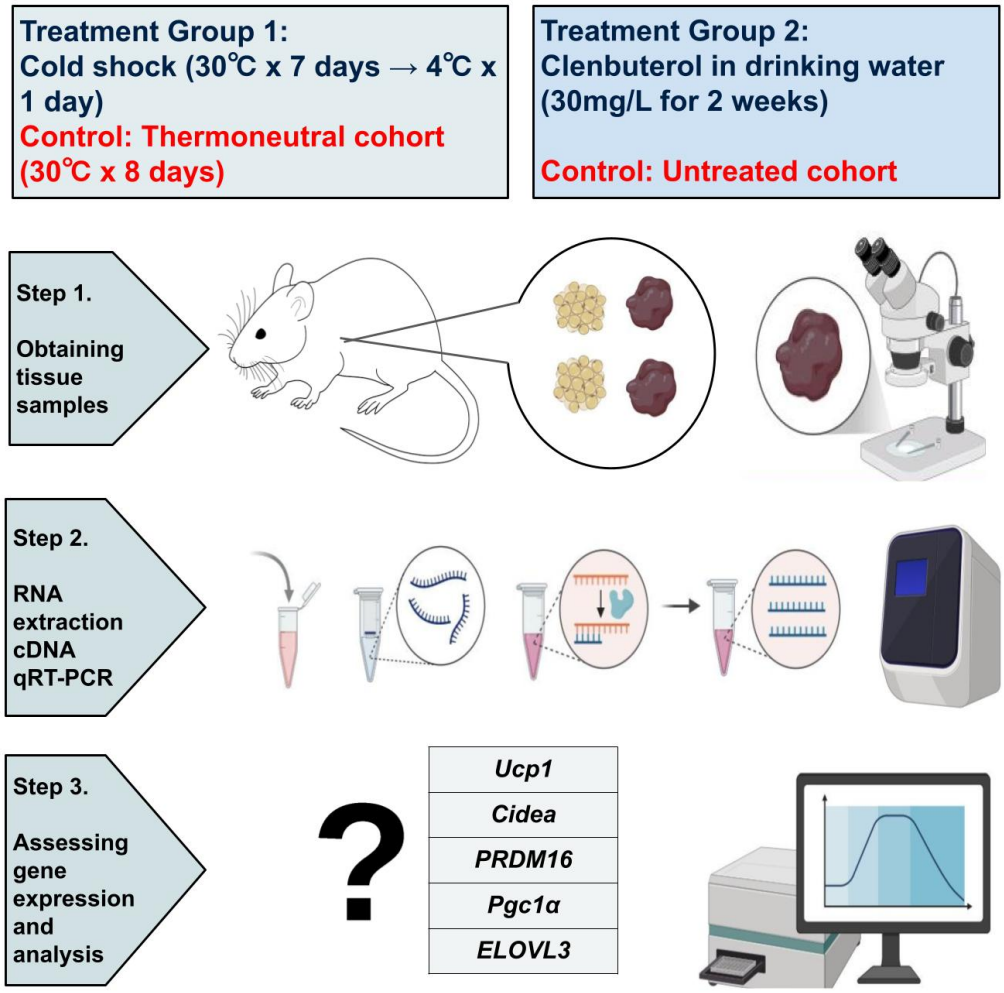


**Figure 5. Experimental induction of BAT thermogenic activation and downstream gene expression analysis.** Mice were subjected to two independent thermogenic stimulation paradigms. Treatment Group 1 underwent cold exposure, consisting of housing at thermoneutrality (30 °C) for 7 days followed by acute cold shock at 4 °C for 24 h; control animals were maintained at thermoneutrality (30 °C) for 8 days. Treatment Group 2 received Clenbuterol (30 mg/L) administered via drinking water for 2 weeks, with untreated animals serving as controls. Following treatment, adipose tissue depots were harvested (Step 1) and processed for RNA isolation. Total RNA was reverse-transcribed to cDNA and gene expression was quantified by qRT-PCR (Step 2). Step 3 involved assessment of thermogenic and brown fat-associated gene expression, including Ucp1, Cidea, Prdm16, Pgc1α, and Elovl3, to evaluate transcriptional responses to cold and pharmacological stimulation.

## 2.5 Rationale for gene selection and validation

The objective was to establish a mechanistically justified panel of thermogenic genes that can help us understand whether pBAT is transcriptionally similar to classical iBAT and how it compares to common WAT depots. Moreover, we were interested in seeing whether

the expression of genes of interest is affected by the cold stimulus/ $\beta_2$-adrenergic stimulation with Clenbuterol.

The selection of genes for transcriptional profiling involved a combination of reviewing existing literature, functional relevance, and depot-specific expression patterns. A minimal, yet complete panel of genes was chosen to capture the full spectrum of processes that define brown adipose biology. These include:

1. **Lineage specification and adipogenic commitment** - *Prdm16* was included as a master regulator of brown adipocyte identity and developmental programming.
2. **Thermogenic machinery and mitochondrial biogenesis** - *Ucp1 (*the hallmark effector of non-shivering thermogenesis) and *Pgc-1α* (a key transcriptional coactivator driving mitochondrial proliferation and oxidative metabolism) were selected to assess the depot's thermogenic potential.
3. **Lipid storage and mobilisation** - *Cidea* and *Elovl3* were included to evaluate the capacity of pBAT to store and mobilize lipids, a crucial aspect of sustained thermogenesis. These genes are also linked to glucose, and fatty acid handling, and their upregulation and high baseline expression indicate that pBAT is metabolically primed to support heat production.

4. **Housekeeping and normalisation** - Using the housekeeping reference gene is essential to ensure reliability of qPCR results and minimize the degree of error that can arise as result of variations between samples, runs, nucleic acid integrity, reverse transcription efficiency, and sample loading amounts. We applied stability testing algorithms (geNorm and NormFinder) to identify a suitable reference gene, *HPRT1*. We have further confirmed its stability across all treatment groups in our pilot experiment. While using multiple reference genes can improve robustness, *HPRT1* is stably expressed across tissues and conditions relevant to thermogenesis, validated in the literature and confirmed stable in our pilot analysis.

| Gene | Full Name | Function/Role in thermogenesis |
|---|---|---|
| *Ucp1* | Uncoupling Protein 1 | Mitochondrial proton transporter that mediates non-shivering thermogenesis; exclusively expressed in BAT. |
| *Cidea* | Cell Death-Inducing DNA Fragmentation Factor Alpha-Like Effector A | Marker of brown adipocytes; regulates lipid droplet formation and is a biomarker of thermogenic activity. |
| *Prdm16* | PR/SET Domain 16 | Transcriptional regulator; drives brown adipocyte differentiation and activates BAT-selective genes. |
| *Pgc-1α* | Peroxisome Proliferator-Activated Receptor Gamma Coactivator 1-Alpha | Master regulator of the thermogenic gene program; promotes mitochondrial biogenesis and oxidative metabolism. |
| *ELOVL3* | Elongation of Very Long Chain Fatty Acids Protein 3 | Involved in fatty acid elongation; contributes to cold-induced thermogenesis and BAT lipid remodeling. |
| *HPRT1* | Hypoxanthine-Guanine Phosphoribosyltransferase 1 | Housekeeping gene used for RT-qPCR normalization, stably expressed in all somatic tissues. |

**Table 1. Summary of Genes Assessed in Thermogenic Profiling.** The thermogenic genes (*Ucp1, Cidea, Prdm16, Pgc-1α,* and *ELOVL3*) were selected based on their well-established roles in brown adipose tissue (BAT) identity and function, as supported by prior literature. *HPRT1* was selected as the reference gene for RT-qPCR normalization due to its consistent and stable expression across a range of somatic tissues and experimental conditions, including those relevant to thermogenic activation in BAT.

## 2.6 Statistical analysis

Statistical differences between two groups were assessed using a two-tailed t-test, while comparisons involving three or more groups were analyzed by one-way ANOVA. The specific statistical tests used, and sample sizes are detailed in the corresponding figure legends. A p-value of less than 0.05 was considered statistically significant. All statistical analyses were conducted using GraphPad Prism 10 and data points presented as Mean ± SEM.

# 3

# Results

## Contents



## 3.1 Tissue Clearing and Immunofluorescence of pBAT

Our findings indicate that pBAT in mice is anatomically integrated with adjacent sympathetic ganglia. Whole-mount immunolabelling of cleared tissue, followed by light-sheet fluorescence imaging, revealed extensive co-localization of tyrosine hydroxylase (TH; marker of sympathetic fibers) and UCP1 (marker of thermogenic adipocytes) within pBAT (Figure 6). TH-positive fibers were observed running longitudinally along the vertebral column and branching into the surrounding tissue, while UCP1-positive adipocyte clusters were found enveloping the sympathetic chain. High integration of sympathetic neurons (Figure 6) with paravertebral BAT highlights a structural and potentially functional coupling driving thermogenic response. The presence of sympathetic input into the pBAT is shown in Figure 7, a high-magnification fluorescence microscopy image that demonstrates the organization of

sympathetic networks within the T2-T4 plexus surrounding pBAT, with neuronal cell bodies and associated processes visible along the paravertebral sympathetic chain, which may provide an anatomical context for sympathetic input to brown adipose tissue.

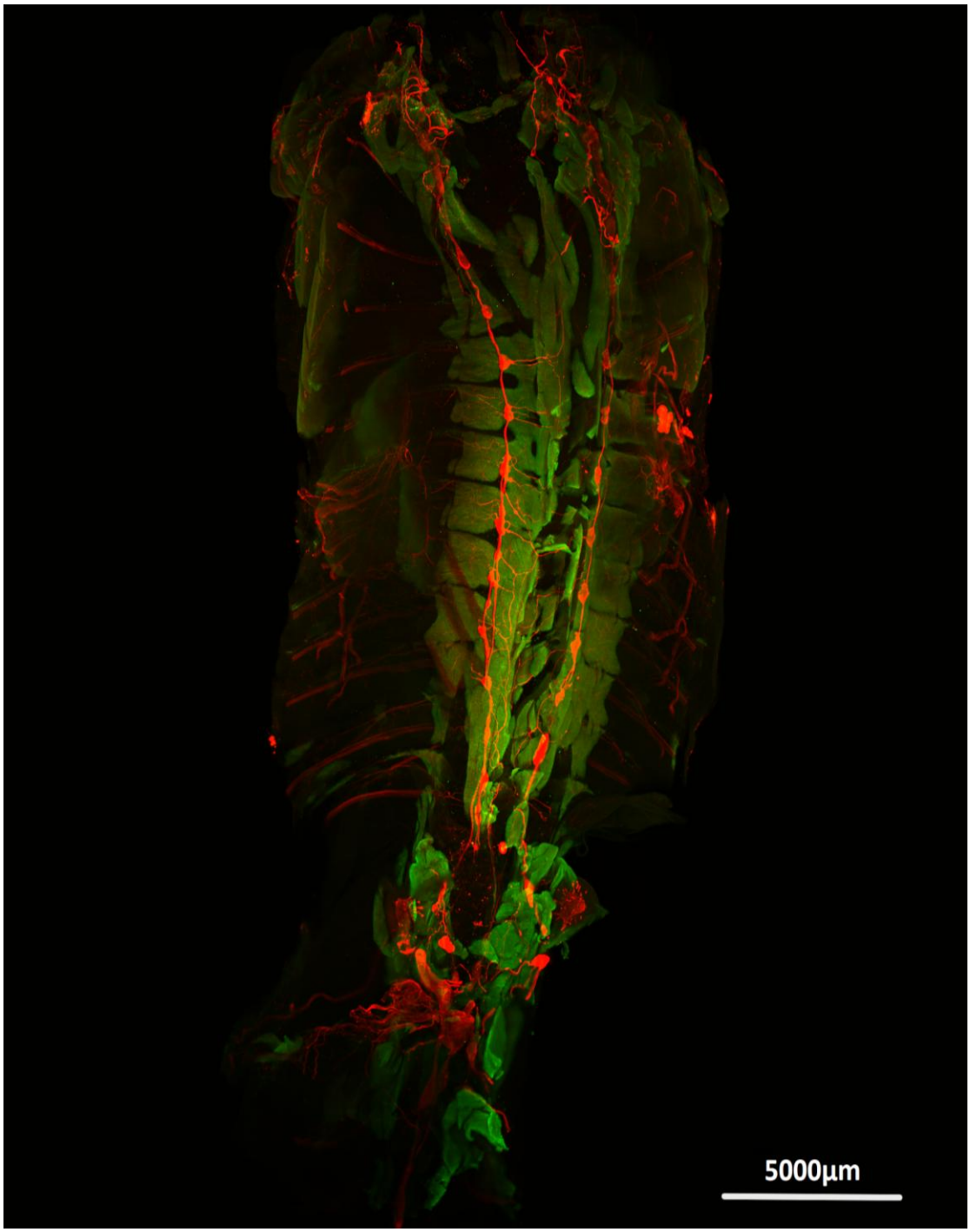


**Figure 6. TH and UCP1 immunostaining image of the paravertebral brown adipose tissue (pBAT) in mice**. Image shows sympathetic fibers and terminals (TH, red), running longitudinally along paravertebral adipose depots and multilocular adipocytes (UCP1, green) in mice exposed to cold (4°C). UCP1-positive structures are clustered around the sympathetic chain, suggesting close anatomical association between brown adipose depots and sympathetic innervation. Scale bar: 5000 µm.


**Figure 7. High magnification image of sympathetic networks in T2-T4 plexus surrounding pBAT.** A high-magnification image of sympathetic chain ganglia acquired using fluorescence microscopy. Neuronal cell bodies are prominently visualized along the paravertebral sympathetic chain, with clearly defined soma, proximal axons, and dendritic projections. This structure underlies the communication between the central nervous system and peripheral targets such as brown adipose tissue. Scale bar: 200 µm

## 3.2 Depot-specific transcriptional profiling of pBAT

Our transcriptional studies compared the BAT signature gene expression across four Below

we describe following:

1. Baseline thermogenic genes expression in thermoneutrality: pilot study (n=1).
2. Thermogenic gene expression in response to natural stimuli (cold) and pharmacological stimulation (Clenbuterol): experimental studies (n=4).

Aligned with previous studies, we have observed significant heterogeneity in gene expression within the depots (Figure 8.A). Notably, pBAT consistently exhibited a more robust thermogenic transcriptional profile, aligned with classical brown fat genetic signature. The recorded alterations in pBAT's gene upregulation surpass those of traditional iBAT, particularly following the acute cold stress (Figure 9A. And B.).

## 3.3 Pilot study: Thermogenic Gene Expression at Thermoneutrality

In this pilot study, we assessed the relative mRNA expression of a thermogenic gene panel across adipose depots in a thermoneutral mouse, using HPRT1 as an endogenous control. The analysis revealed apparent depot-dependent differences, with pBAT exhibiting the highest *Ucp1* expression (Figure 8A). As shown in Figure 8B, expression of core thermogenic genes was prominent in pBAT. *Ucp1* and *Pgc-1α* expression appeared higher in pBAT compared with classical iBAT, whereas *Cidea* and *Elovl3* levels were comparable between the two depots. In contrast, *Prdm16* expression appeared lower in pBAT relative to iBAT. Overall, the expression profiles of thermogenic genes in pBAT more closely resembled those of iBAT than white adipose tissue depots. Given the limited sample size (n = 1), statistical analysis was not performed, and the data are presented as representative observations to assess the detectability of genes of interest in pBAT.

Collectively, these findings established the presence of these BAT-characteristic markers in pBAT, particularly high *Ucp1* expression, and were sufficient for us to pursue further experiments assessing its responsiveness to both physiological (cold exposure) and pharmacological ($\beta_2$-adrenergic stimulation) activation.

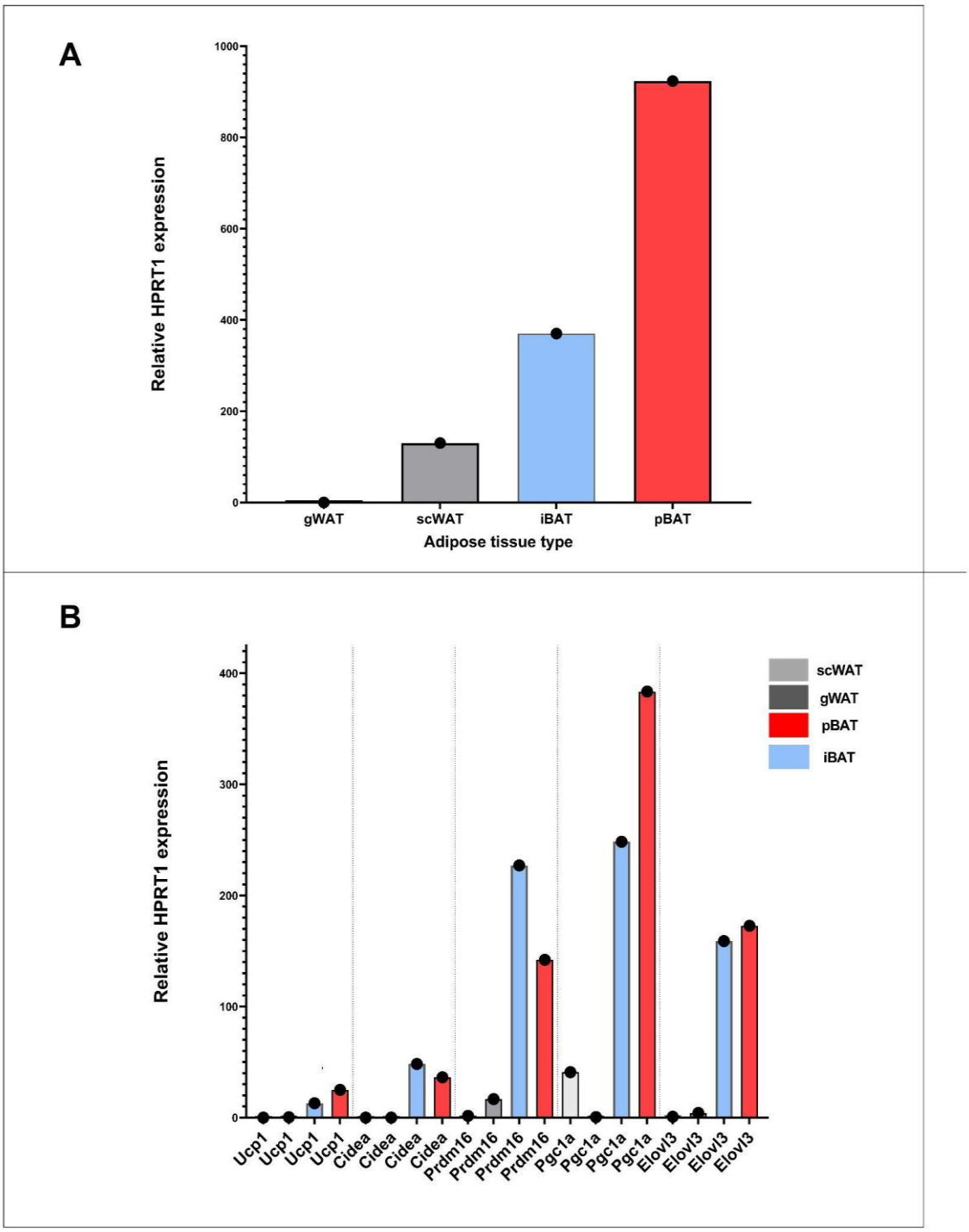


**Figure 8. Pilot study results.**

**(A) Relative fold expression of *Ucp1* in pBAT compared to the iBAT and white adipose tissue depots.** This graph represents a pronounced difference in Ucp1 expression between depots, highest being pBAT (red). Gene expression has been assessed against the endogenous control gene *HPRT1*.

**(B) Relative expression of thermogenesis-associated genes across adipose depots of thermoneutral mice.** We observed striking upregulation of thermogenesis-associated genes in pBAT (red) as compared to iBAT (blue) and WAT depots (in grey), all groups were compared to a single control group (iBAT). No statistical analysis was performed on these graphs, due to the sample size (n=1), instead data served as representative observation.

## 3.4 Cold Stress: Thermogenic Genes Strongly Upregulated in pBAT

### UCP1

Animals exposed to acute cold shock (24h) exhibited a robust upregulation of *Ucp1* mRNA expression in paravertebral BAT (pBAT), with a ~550-fold increase compared to thermoneutral controls ($p < 0.0001$) (Figure 9.A). By contrast, interscapular BAT (iBAT) showed less robust, though still significant, 17-fold induction under the same conditions ($p = 0.0024$) (Figure 9.A). Visibly, there was a significant difference between iBAT and pBAT, as shown on Figure 9.B. To determine whether the markedly greater fold-change observed in pBAT could be attributed to differences in basal *Ucp1* levels between depots, we assessed *Ucp1* expression at thermoneutrality (performed on the background, not graphically presented in this thesis). Baseline *Ucp1* expression did not significantly differ between pBAT and iBAT ($p = 0.6046$). Thus, the exaggerated cold-induced response in pBAT reflects a true depot-specific amplification of *Ucp1* induction rather than differences in starting expression levels.

### Pgc-1α

Following cold shock, pBAT demonstrated a ~2440-fold increase in *Pgc-1α* expression compared to thermoneutral controls ($p < 0.0001$) (Figure 9.C). *Pgc-1α* is a key transcriptional coactivator regulating mitochondrial biogenesis and oxidative metabolism, and its robust induction in pBAT is consistent with an expansion of mitochondrial content and enhanced oxidative capacity in this depot.

### Elovl3

Similarly, pBAT demonstrated a ~62-fold increase in *Elovl3* expression ($p = 0.0016$) compared to thermoneutral controls (Figure 9.C). Interestingly, iBAT showed an even greater induction of *Elovl3* (~142-fold) (Figure 9.A). Since *Elovl3* encodes an enzyme involved in

very-long-chain fatty acid elongation and is tightly linked to thermogenic lipid metabolism, this suggests that iBAT may rely more heavily on lipid remodeling as part of its adaptive response to acute cold exposure.

**Cidea**

In contrast, *Cidea* expression was upregulated to a similar extent in both depots (~71-fold in pBAT vs. ~60-fold in iBAT; p=0.007 and p=0.001, respectively) (Figure 9.A and 9.C). *Cidea* is associated with lipid droplet formation and regulation of lipolysis, as well as negative regulation of *Ucp1*. These results indicate that cold stress promotes a comparable enhancement of lipid storage and internal regulatory machinery in both pBAT and iBAT.

**Prdm16**

Cold shock resulted in a 13-fold increase ($p < 0.003$) in the expression of the master transcriptional regulator *Prdm16* in pBAT (Figure 9.C), which was comparable to the 18-fold increase observed in iBAT (p=0.0012) (Figure 9.A).

To summate, we examined the expression of key BAT genes under thermoneutral (30°C) and cold exposure (4°C) conditions. Cold exposure caused a dramatic increase in thermogenic genes in pBAT depot compared to other adipose depots (Figure 9.B). Importantly, *Ucp1* expression in pBAT increased by roughly 550-fold upon cold shock, compared with thermoneutral controls ($p < 0.0001$). Other core BAT-associated genes showed a positive trend as well, with *Cidea*, *Prdm16*, *Pgc-1α*, and *ELOVL3* all significantly upregulated ($p < 0.001$ to $p < 0.01$) (Figure 9.A and 9.C). These genes are known to regulate mitochondrial function, lipid metabolism, and brown adipocyte identity, suggesting a coordinated robust, transcriptional response to cold.

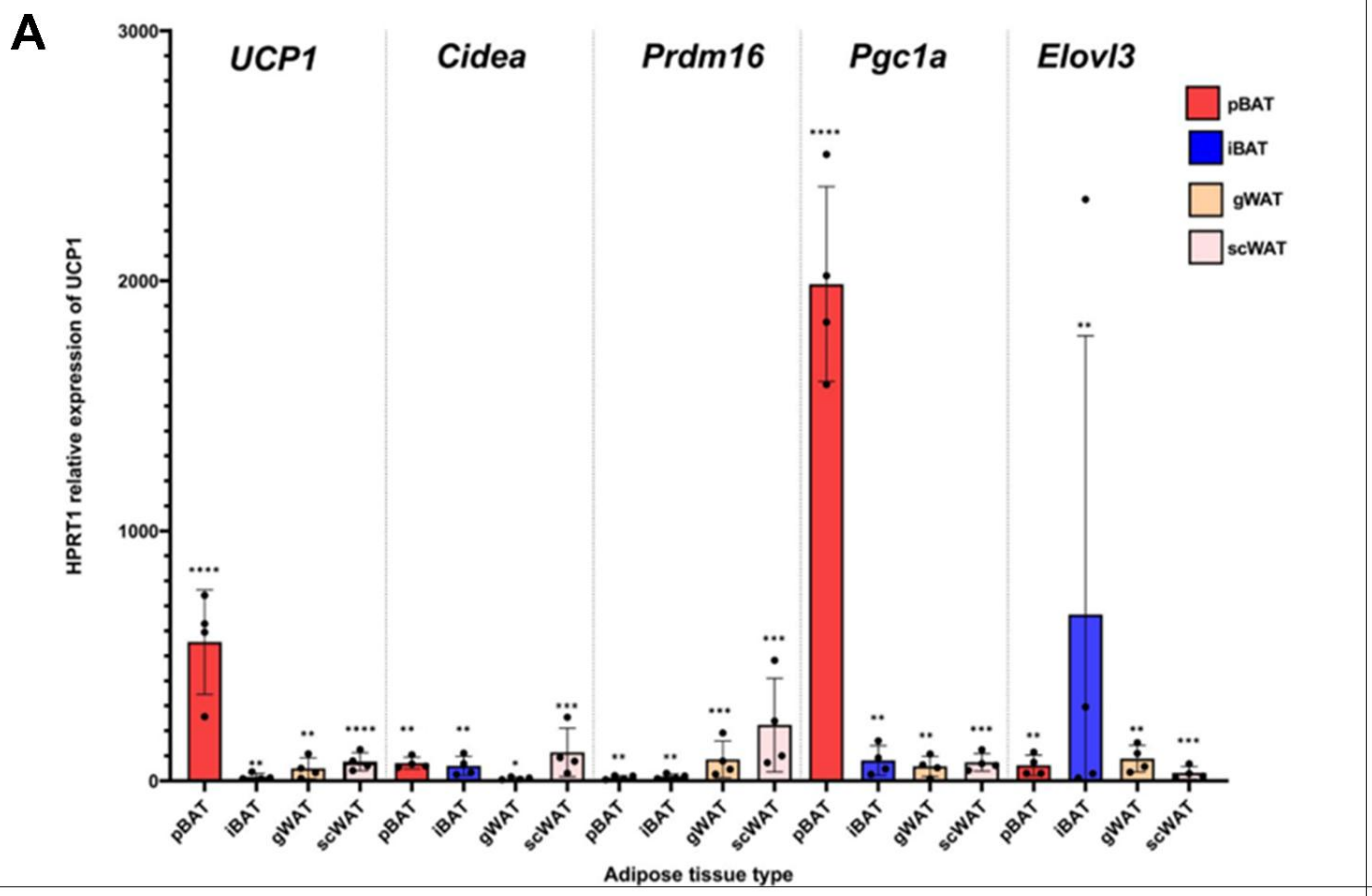
A
UCP1
Cidea
Prdm16
Pgc1a
Elovl3
pBAT
iBAT
gWAT
scWAT
HPRT1 relative expression of UCP1
3000
2000
1000
0
Adipose tissue type

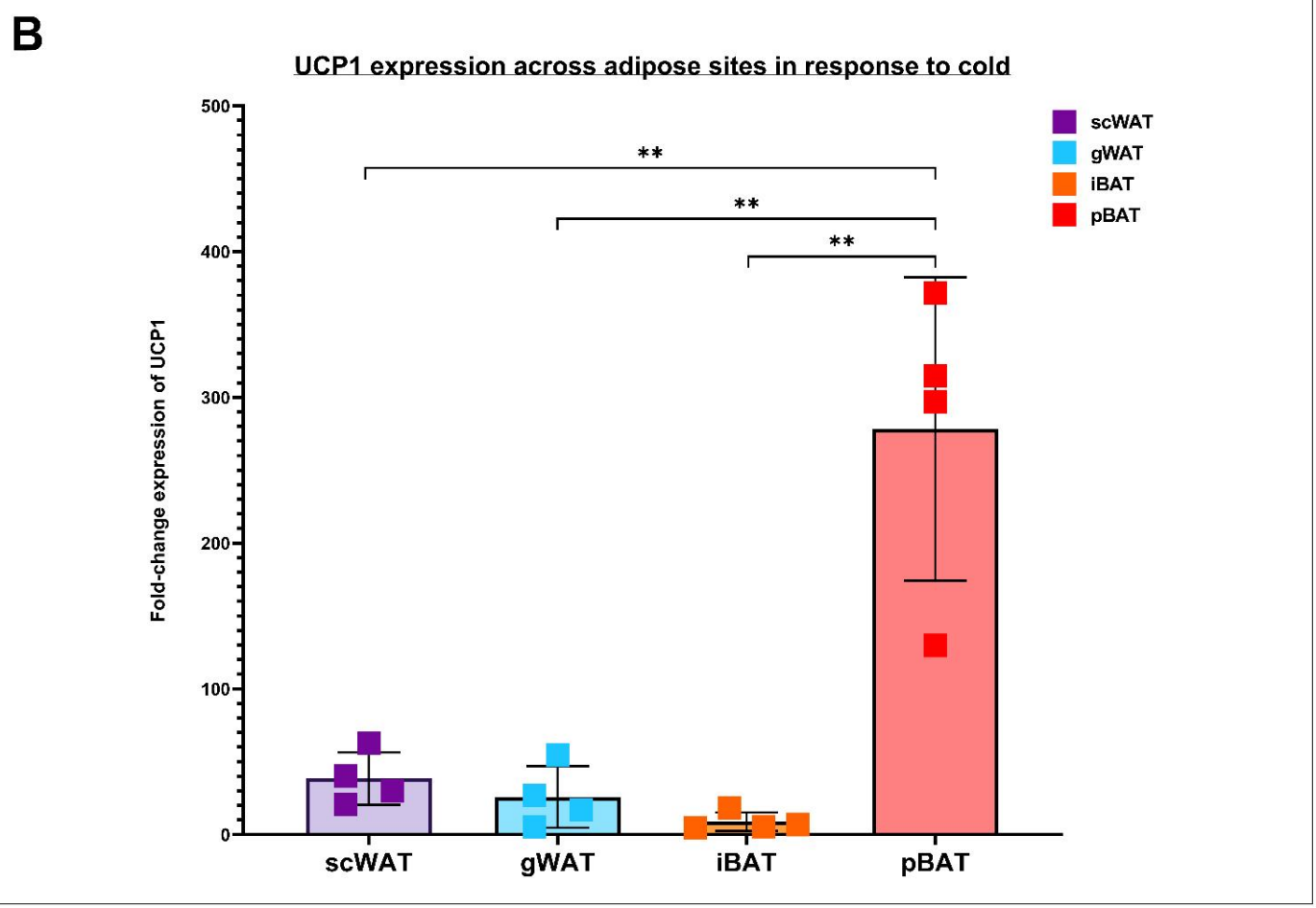
B
UCP1 expression across adipose sites in response to cold
scWAT
gWAT
iBAT
pBAT
Fold-change expression of UCP1
500
400
300
200
100
0
**
**
**

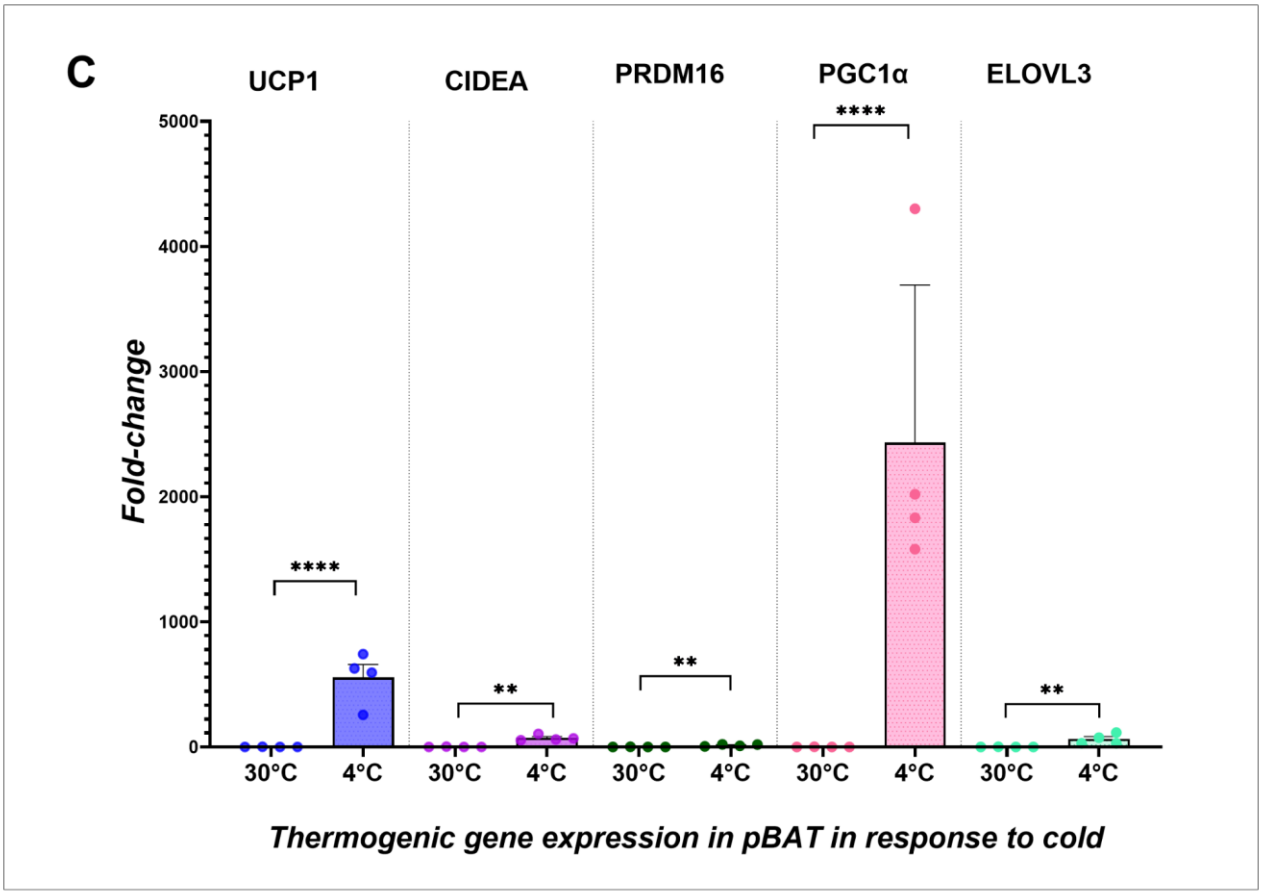


**Figure 9. Cold exposure induces depot-specific thermogenic gene expression in mouse adipose tissue.**

**(A)** Relative mRNA expression of thermogenic and mitochondrial genes (*Ucp1*, *Cidea*, *Prdm16*, *Pgc-1a*, and *Elovl3*) in mouse paravertebral brown adipose tissue (pBAT, red), interscapular brown adipose tissue (iBAT, blue), gonadal white adipose tissue (gWAT, yellow), and subcutaneous white adipose tissue (scWAT, beige). pBAT exhibited a ~550-fold increase in *Ucp1* expression (****p = 0.00003) compared to ~17-fold increase in iBAT(**p = 0.0024). Interestingly, compared to thermoneutral controls pBAT showed high expression of *Cidea (**p=0.007), Prdm16(**p<0.003), Pgc-1α* ~2440-fold (****p < 0.0001) and *Elovl3 (**p* = 0.0016). Bars represent mean ± SEM with individual biological replicates shown (n = 4). Statistically significant differences as determined by one-way ANOVA with Tukey's post-hoc testing.

**(B)** Fold-change in Ucp1 expression following cold exposure across mouse adipose depots. This section demonstrates increased expression of *Ucp1* in pBAT upon cold shock (4°C, 24h), particularly in comparison to classical iBAT. Results confirmed that pBAT exhibits significantly higher Ucp1 expression compared to iBAT *(**p = 0.002*), gWAT (**p = 0.004), and scWAT (**p = 0.0032).Bars present mean ± SEM with individual biological replicates shown (n = 4).Statistical significance was determined using unpaired Student's t-tests for pairwise comparisons between pBAT and each depot.

**(C)** Thermogenic gene expression in mouse pBAT under thermoneutral (30 °C) and cold-exposed (4 °C) conditions. This panel shows fold-change mRNA expression relative to thermoneutral controls (all values same as stated in Section A). Bars represent mean ± SEM with individual biological replicates shown (n = 4). Statistically significant differences as determined by one-way ANOVA with Tukey's post-hoc testing. For all panels illustrated above significance is indicated as: ns (non-significant), p < 0.05 (*), p < 0.01 (**), p < 0.001 (***), and p < 0.0001 (****).

## 3.5 β-adrenergic stimulation of pBAT with Clenbuterol

Pharmacological stimulation with the $\beta_2$-adrenergic agonist Clenbuterol further supported pBAT's capacity to upregulate the thermogenic gene expression. Stimulation of $\beta_2$-ARs in treated mice resulted in a similar effect on both classical iBAT depot and pBAT, showing statistically strong upregulation of *Ucp1* and *Cidea*, however, not the remaining genes (e.g *Pgc-1α*, *Elovl3*, *Prdm16*) as shown explicitly in Figure 10.A. Potential reasons underlying these trends will be discussed in greater detail in the **4. Discussion** section.

**UCP1**

As presented in Figure 10.A and 10C. mice treated with Clenbuterol showed a 60-fold increase in pBAT's *Ucp1* expression ($p < 0.0001$), which is 3-fold greater relative to 20-fold change observed in iBAT ($p = 0.0011$). We have compared the baseline expression of *Ucp1* in both depots under no treatment to understand whether there is a significant treatment-associated effect, which showed that under no treatment, both tissues exhibit similar *Ucp1* expression, with no statistically significant difference between depots. This highlights pBAT's ability to respond to sympathetic input.

**Cidea**

Along with *Ucp1*, we have observed a strong upregulation of *Cidea* following the treatment (Figure 10.A). Levels of *Cidea* expression following the treatment were similar between pBAT and classical iBAT depot, with the mean fold change of 80 ($p = 0.0001$) and 75 ($p = 0.0023$), respectively.

Collectively, these results show a degree of pharmacological induction of thermogenic gene transcription in pBAT. While the thermogenic response across all depots was less pronounced compared to cold challenge, pBAT still exhibited notable upregulation of the hallmark thermogenic marker *Ucp1*. In treated mice, *Ucp1* expression in pBAT was significantly greater than in classical iBAT and scWAT depots (Figure 10.B).We have noticed visually evident upregulation in *Pgc-1α*, *Elovl3*, and *Prdm16* mRNA levels following the treatment, however

these changes did not reach statistical significance (Figure 10.C).

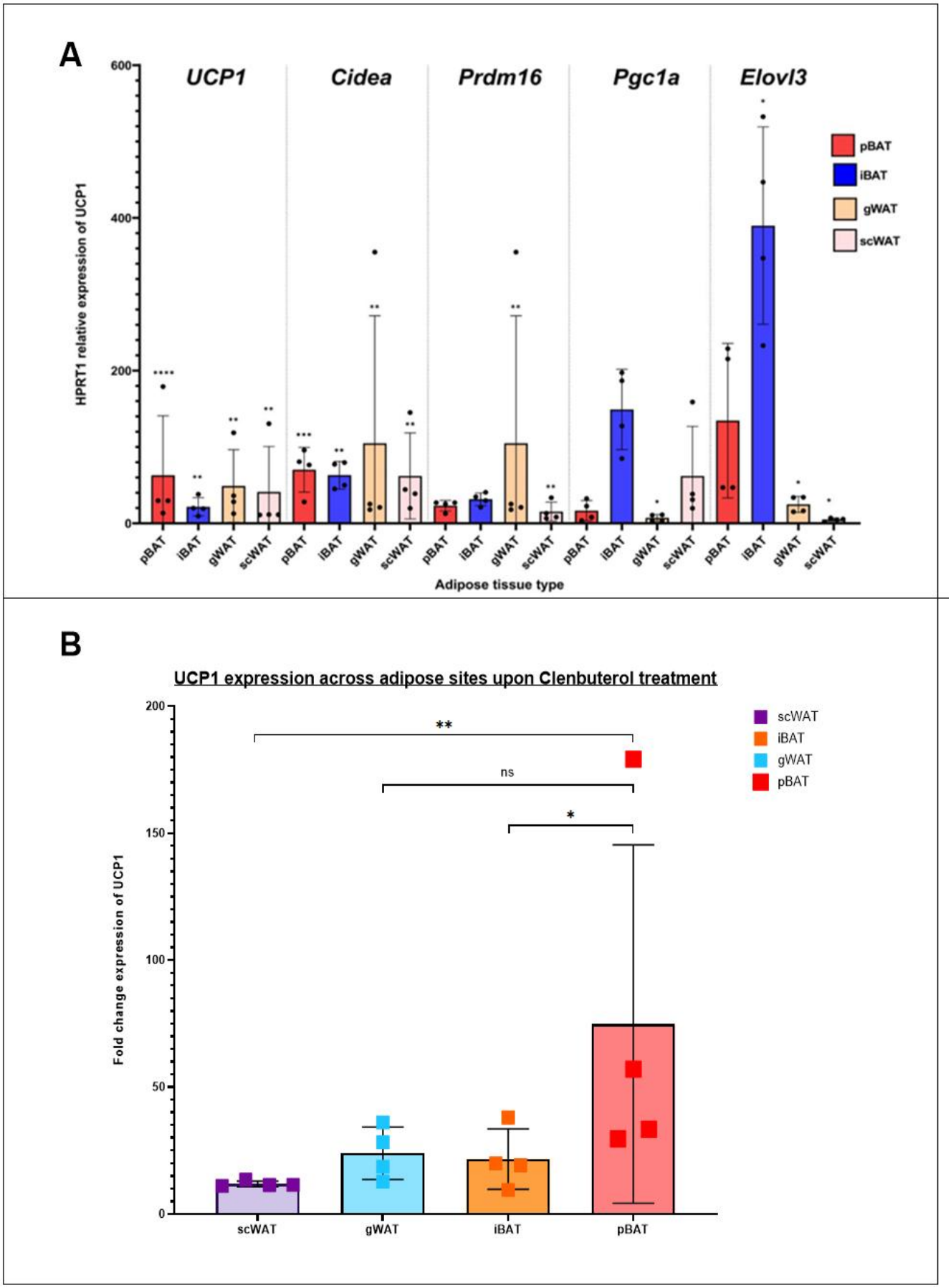

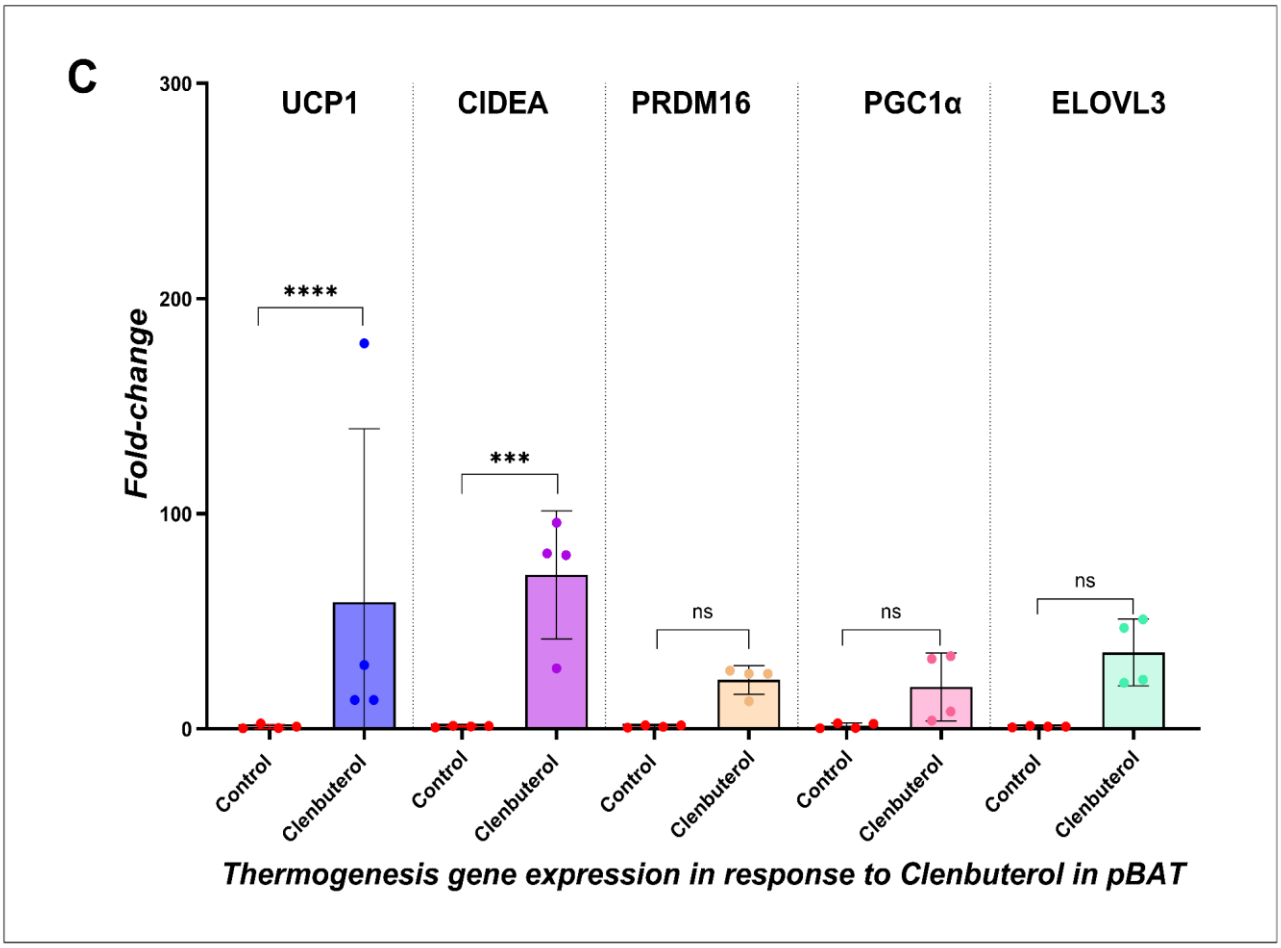


**Figure 10. Effect of Clenbuterol on depot-specific thermogenic gene expression in mouse adipose tissue.** **(A)** Relative mRNA expression of thermogenic genes (*Ucp1*, *Cidea*, *Prdm16*, *Pgc-1a*, and *Elovl3*) in mouse paravertebral brown adipose tissue (pBAT, red), interscapular brown adipose tissue (iBAT, blue), gonadal white adipose tissue (gWAT, yellow), and subcutaneous white adipose tissue (scWAT, beige). Clenbuterol promotes expression of *Ucp1 (****p < 0.0001)* and *Cidea (***p = 0.0001)* in pBAT. Similarly, in iBAT β-adrenergic stimulation, caused statistically relevant upregulation in *Ucp1 (**p =0.0011), Cidea (**p = 0.0023), Elovl3 (*p =0.08)*. Bars represent mean ± SEM with individual biological replicates shown (n = 4). Statistically significant differences were determined by one-way ANOVA with Tukey's post-hoc testing.

**(B)** *Ucp1* expression across paravertebral (red), subcutaneous (purple), gonadal (blue), and interscapular (orange) adipose depots in response to Clenbuterol. Following the treatment, *Ucp1* expression in pBAT depot was significantly higher than scWAT*(**p < 0.005)* and iBAT *(*p < 0.01)*, but not gWAT (ns).Bars present mean ± SEM with individual biological replicates shown (n = 4).Statistical significance was determined using unpaired Student's t-tests for pairwise comparisons between pBAT and each depot.

**(C)** This panel focuses on solely pBAT's relative mRNA expression of *Ucp1*, *Cidea*, *Prdm16*, *Pgc-1a*, and *Elovl3,* and expressed as fold-change relative to no treatment controls. This panel underlines *Ucp1(****p < 0.0001)* and *Cidea (***p =0.00018)* being upregulated in pBAT, but not other assessed genes in response to Clenbuterol. Bars present mean ± SEM with individual biological replicates shown (n = 4)**.** Statistical significance was assessed using one-way ANOVA Tukey's post-hoc testing. For all panels illustrated above significance is indicated as: ns (non-significant), $p < 0.05$ (*), $p < 0.01$ (**), $p < 0.001$ (***), and $p < 0.0001$ (****).

# 4

# Discussion

## Contents



## 4.1 General Discussion

In this chapter, I will place the overall findings of this thesis within the broader context of the field, considering how they extend current models of BAT heterogeneity and highlight potential directions for future investigation.

In the light of the escalating global obesity epidemic and associated metabolic diseases, the possibility of therapeutic BAT activation is particularly compelling. At present, targeting BAT remains elusive, as a knowledge gap persists regarding the existence of a true human equivalent of the classical interscapular adipose tissue, iBAT. Although iBAT is the most well-studied thermogenic BAT depot essential for thermoregulation and survival in

endotherms, it has no translational application, as in humans, iBAT is only active in infants and gradually undergoes age-dependent degeneration.

This research thus investigated the transcriptional profile of a previously overlooked paravertebral BAT, pBAT, depot that is present in both small mammals, such as mice, as well as adult humans. Our study focuses on the thermogenic potential of pBAT in mice. We investigated the expression of BAT-specific genes in response to 1) cold exposure and 2) $\beta_2$ agonist, Clenbuterol. For a fuller comparative analysis, we have evaluated alongside those of different adipose tissue depots, particularly classical thermogenic site, iBAT.

Our findings reveal an intriguing observation that pBAT from C57BL/6J mice express a robust brown fat gene signature at thermoneutral conditions, with strong upregulation of *Ucp1*, *Cidea*, *Elovl3*, *Prdm16*, and *Pgc-1α* at levels comparable to classical iBAT (Figure 8). The presence of this pronounced thermogenic transcriptional profile in absence of external stimulus (e.g. cold) could reflect background sympathetic tone activation and suggest that pBAT exists in a pre-activated or constitutively primed state. Since pBAT is positioned in anatomical proximity to the spinal cord and sympathetic chain, it's plausible that this pre-activated state is maintained to ensure adequate level of thermoprotection of neural structures and sustaining of efficient sympathetic outflow during ambient cold exposure. Evidence from rodents and hibernating mammals shows pBAT's role in countercurrent heat exchange, warming neurovascular structures and vital body organs, therefore providing localised protection against cold (Smith, 1964).

Our immunohistochemistry imaging analysis reveals presence of sympathetic networks closely associated with pBAT (Figure 7). Consistent with the recognised role of the sympathetic nervous system in BAT thermogenesis, we observed sympathetic activation of the region with close spatial association of UCP1 and TH in mice exposed to cold (Figure 6). This demonstrates active sympathetic input into the tissue and suggests this depot

operates under strong autonomic control, potentially facilitating the induction of a brown adipose thermogenic program upon relevant environmental cues.

More interestingly, our further findings confirm these views by showing that pBAT is responsive to both environmental stimuli with cold, and pharmacological treatment with Clenbuterol. The level and strength of upregulation between these two stimuli varied, with cold being a more robust activator of the BAT transcriptional profile in both pBAT and iBAT. This was expected as cold elicits a multi-layered neuro-endocrine cascade targeting numerous intracellular pathways, while Clebuterol activates a narrower intracellular pathway, primarily cAMP-PKA-CREB, without engaging the full network of co-signals that amplify thermogenesis.

The transcriptional profile of pBAT in both instances was aligned with the traditional activation of truly brown adipose tissue. Surprisingly, we detected a higher level of thermogenic activation in pBAT compared to iBAT in numerous instances and looked further into these changes to understand variability in both depots. Among other differences, pBAT demonstrated dramatic upregulation of early transcriptional activator gene *Pgc-1α* and effector gene, *Ucp1*, exceeding iBAT significantly (Figure 9.A and 9.C). These two genes are important for early response and rapid initiation of oxidative uncoupling, suggesting that pBAT potentially plays a role as a rapid-response thermogenic depot distinct from iBAT by virtue of its heightened sensitivity and regulatory flexibility. Further studies of pBAT are essential to validate these views and assess the magnitude of pBAT's thermogenic response.

Overall, these findings depict that pBAT in mice exhibits a pronounced thermogenic transcriptional profile, supporting the view that this depot is functionally primed for rapid thermoregulatory activation. The elevated baseline expression of key brown fat genes shown in Figure 8.A, suggests that pBAT may contribute to early or tonic thermogenic

responses, rather than serving solely as a reserve activated under acute environmental challenge. The following sections provide a comprehensive description and interpretation of the experimental findings.

## 4.2 pBAT expresses classical brown fat program: pilot study

To verify the feasibility of this approach, we first checked whether pBAT of C57BL6/J WT mice exhibited any genetic markers of thermogenesis under normal conditions (room temperature, without environmental or physiological stimuli). By conducting a pilot study, we found that mice kept at thermoneutral conditions showed robust *Ucp1* expression (Figure 8.A), along with increased levels of *Cidea, Elovl3, Prdm16*, and *Pgc-1α* (Figure 8.B), which reflect the canonical gene signature of classic iBAT, and distinguishes pBAT from white adipose depots.

Each of these genes plays a critical role in sustaining brown fat function: *Ucp1* in uncoupled respiration, *Cidea* in lipid droplet dynamics and negative control of *Ucp1*, *Elovl3* in fatty acid metabolism, and *Prdm16* and *Pgc-1α* in transcriptional regulation and mitochondrial biogenesis. Expression of these genes at basal conditions is not typical for inducible dormant white adipose depots, whereas it is constitutive and robust in thermogenic BAT depots (Fitzgibbons et al., 2011; Seale, 2015). Having established the notable upregulation of brown fat-specific genes in pBAT of WT mice at levels comparable/exceeding classical iBAT depot, we next conducted planned experimental studies.

## 4.4 pBAT: Cold-Stimulus

Firstly, we were able to identify a strong positive correlation between the decrease in the environmental temperature and upregulation of pBAT's genes associated with non-shivering thermogenesis. Most importantly, this study has confirmed the hypothesis that at

baseline pBAT's gene expression resembles characteristics of classic brown adipocytes and is highly responsive to adrenergic stimulation.

Standard "room temperature" (around 20-22 °C), induces mild cold stress for mice because of their small body size, high surface area-to-volume ratio and poor insulation. Therefore, at this range they rely on brown adipose tissue to activate non-shivering thermogenesis to maintain core body temperature. To reduce this background BAT activity, we acclimatised the mice to thermoneutrality (~30 °C) for a week before the experiment. This preconditioning allowed us to silence baseline thermogenic expression, giving us a clearer baseline from which to detect transcriptional changes triggered specifically by the temperature drop.

Indeed, acute cold shock (~24h) revealed striking transcriptional change in pBAT depot, which I believe resulted from sympathetic-driven transcriptional activation. Exposure to cold resulted in a pronounced induction of *Ucp1*, *Pgc-1α*, *Cidea*, *Elovl3* and modern upregulation of *Prdm16* genes in pBAT (Figure 9. C).

Importantly, the key marker, *Ucp1*, was dramatically upregulated, with expression levels increasing by nearly 550-fold relative to the thermoneutral baseline (Figure 9. C). This magnitude of induction reflects the functional "switching on" of BAT, as UCP1 is the central effector of non-shivering thermogenesis, uncoupling oxidative phosphorylation to generate heat.

We have found that the response in pBAT was markedly greater than that observed in other adipose depots. Classical iBAT, long regarded as the primary thermogenic depot in rodents, exhibited robust *Ucp1* induction (17-fold change to baseline), but to a substantially lower degree compared to pBAT (Figure 9. B). Indeed, pBAT upregulation exceeded iBAT by approximately 32-fold under identical cold exposure, suggesting depot-specific differences in sympathetic innervation or transcriptional responsiveness. Furthermore, the magnitude of

*Ucp1* induction in pBAT also surpassed that observed in inducible beige adipocytes within subcutaneous and gonadal white adipose depots (Figure 9. B), underscoring the distinctive thermogenic potential of this tissue. This ultimately reflects that pBAT has capacity to protect surrounding tissues and vital organs from cold stress. To ensure the validity of this comparison, we have ensured that baseline levels were comparable across all assessed tissues and showed no statistically significant difference.

Another important observation was the marked induction of the *Pgc-1α* gene in pBAT (Figure 9. A). Interestingly, the expression *Pgc-1α* has been prominent in both iBAT and pBAT, but to a much lesser degree in WAT. Shown in Figure 9.A, the magnitude of the *Pgc-1α* upregulation was the highest among all candidate genes analyzed (with over 2000-fold change compared to thermoneutral controls). Given the specific regulatory role of Pgc-1α, we believe it could be because a boost in *Pgc-1α* mRNA precedes and supports full activation of the downstream thermogenic genes.

These findings are consistent with the existing literature which specifically highlights the role of *Pgc-1α* as an early transcriptional regulator of downstream thermogenic effector genes that boosts oxidative capacity of BAT. *Pgc-1α* orchestrates induction of numerous BAT genes and acts as a transcriptional coactivation of nuclear receptors, such as PPARγ. This occurs downstream of cAMP-PKA-CREB signaling, ultimately leading to increased cellular content of mitochondrial DNA, boosting mitochondrial biogenesis and facilitating the ability of the cell to oxidase fatty acids and glucose (Fernandez-Marcos and Auwerx, 2011). This high induction observed in pBAT following the acute cold shock most likely reflects that our sampling coincided with the window of maximal gene activation, which is reported to occur 6-24 hours following acute cold stimulation (Fernandez-Marcos and Auwerx, 2011). High responsiveness of the pBAT to sympathetic activation, and capacity to rapidly upregulate this gene highlights that its transcriptional profile resembles classical BAT in its nature (Puigserver et al.,1998).

Highly thermogenic BAT relies heavily on lipolysis-derived fatty acids, which serve as a primary fuel for heat generation (Klingenspor, 2003). The ability of the tissue to store, recruit and mobilise lipids intracellularly is key to ensuring sufficient substrate availability and oxidation to sustain timely thermogenic response (Vegiopoulos and Herzig, 2007). This functional requirement is reflected in BAT's transcriptional profile, which usually includes high expression of genes involved in lipid droplet dynamics and fatty acid metabolism (Wang et al., 2022). Among these are two genes that were included in our analysis, namely *Cidea* and *Elovl3*.

In our observations, lipid metabolism pathways were upregulated in pBAT, presenting a 60-fold increase in *Elovl3* expression (Figure 9. A). Previous studies revealed modest baseline expression of *Elovl3* at baseline, regulated by systemic factors such as glucocorticoids, which however, can be robustly induced by adrenergic signaling or in response to cold (Vegiopoulos and Herzig, 2007). Its protein product catalyses fatty acid elongation, which is essential for meeting the energy demands of enhanced fatty acid oxidation in activated brown adipocytes. Importantly, *Elovl3* activity is essential even before cold exposure, likely preparing the tissue for efficient thermogenic response when needed.

Furthermore, the inability of *Elovl3*-deficient mice to fully activate their brown fat after prolonged cold exposure reinforces the idea that *Elovl3* expression is essential not only during initial recruitment but also necessary for maintaining optimal BAT function under thermogenic stress (Westerberg et al., 2006). Interestingly, we observed higher expression of *Elovl3* in the classical iBAT depot (Figure 9A). In contrast, *Ucp1* and *Pgc-1α* levels remained relatively low, which may suggest that iBAT had not yet reached full thermogenic activation. This pattern could reflect a preparatory or priming stage, where lipid metabolism pathways are upregulated in anticipation of subsequent thermogenic demand, while pBAT exhibits maximal induction

In parallel, I have observed high expression of *Cidea*, with transcript levels being similar in classic iBAT and pBAT, 60 and 72, respectively (Figure 9A). The slightly higher expression in pBAT is noteworthy, it could mean that pBAT has good ability for lipid droplet formation and stabilisation - a critical process for effective storage of energy substrate for thermogenic activation. Beyond its role in lipid storage, *Cidea* also functions as a negative regulator of Ucp1 activity, fine-tuning thermogenic output to prevent excessive energy expenditure. The similar expression of *Cidea* in pBAT and iBAT suggests that, despite pBAT's higher overall thermogenic gene expression, its activity is likely tightly controlled, maintaining a balance between maximal energy mobilization and homeostatic regulation. Taken together, these findings indicate that pBAT possesses both a highly inducible thermogenic program and the molecular machinery to manage efficient downregulation of these genes and prevent overactivation.

Lastly, the *Prdm16* gene, a master transcriptional regulator of BAT identity, showed a 13-fold increase in pBAT, and similarly, an 18-fold increase in iBAT (Figure 9A). While being slightly higher in iBAT, no significant difference in gene expression between these two sites has been observed. These further highlights that both sites activate similar regulatory programs in response to cold. Additionally, this could mean that any discrepancies in downstream thermogenic effectors that were observed in this study are likely not driven by differences in *Prdm16*.

## 4.5 pBAT: β-adrenergic stimulation with Clenbuterol

Our choice of treatment with Clenbuterol was based on the observation that sympathetic neurons innervating iBAT express $\beta_2$AR, suggesting that pharmacological activation could directly stimulate these neurons and, in turn, drive thermogenic gene expression in the tissue (Cheung et al., 2025). Based on these findings, we wanted to know whether

sympathetic neurons innervating pBAT express $\beta_2$AR in similar way and assess the responsiveness of paravertebral depot to Clenbuterol treatment.

Despite this notion, we have anticipated a lower magnitude of the response, as thermogenesis in rodents is primarily mediated through $\beta_3$AR-signaling. Even if the sympathetic neurons innervating pBAT express $\beta_2$AR, it was difficult to predict the strength and effectiveness of downstream signaling cascade triggered by pharmacologic $\beta_2$-adrenergic stimulation.

As anticipated, pharmacological stimulation with selective $\beta_2$-adrenergic receptor agonist did not produce the same level of transcriptional activation in pBAT (Figure 10.B). We observed only partial induction of thermogenic genes, with *Ucp1* and *Cidea* being upregulated (Figure 10.C), whereas key transcriptional regulators such as *Pgc-1α*, *Prdm16*, and *Elovl3* showed no statistical difference compared to the controls (Figure 10.A). This pattern likely represents a selective activation of immediate effector genes, but not the whole thermogenic networks in BAT.

The concurrent upregulation of *Ucp1* and *Cidea* indicates induction of the mitochondrial uncoupling machinery, alongside its intrinsic control. Expression of *Ucp1* showed 60-fold increase in BAT of Clenbuterol-treated mice, threefold higher than the 20-fold increase observed in the classical iBAT depot (Figure 10.A). *Cidea* mRNA levels in treated mice were comparable in two depots, with an 80-fold change in pBAT and 75-fold change in iBAT (Figure 10.A). As reported in prior studies, it is not surprising that β-adrenergic agonism causes a lower degree of induction compared to cold exposure. Several factors specific to our study may account for this outcome, as described below.

Our study results align with previous studies that report smaller or more focused changes in gene expression following β-agonist treatment than after cold, particularly for genes involved in mitochondrial biogenesis, lipid droplet remodeling and whole-tissue remodeling

(Qin et al., 2015; Li et al., 2021). This likely reflects differences in receptor subtype engagement, duration and pattern of sympathetic activation, and systemic co-signals elicited by cold. Cold elicits a broad, multi-layered sympathetic and endocrine response that simultaneously activates multiple signaling and transcriptional programs, leading to activation of several types of adrenergic receptors, including $\beta_3$AR.

The observed lack of induction of upstream transcriptional regulators, such as *Pgc-1α* and *Prdm16* in this study could be due to insufficient adrenergic strength, or limited pharmacokinetics of the drug delivered in drinking water. While Clenbuterol mimics one component of sympathetic activation, cold exposure triggers a coordinated network of signaling pathways, enhancing both acute and sustained thermogenic capacity in pBAT.

## 4.6 Comparative analysis of pBAT and white adipose tissues

Lastly, we aimed to compare the transcriptional profiles of pBAT and white adipose tissue depots, focusing on the most prevalent WAT depots in mice: scWAT and visceral gWAT. ScWAT is known to undergo adaptive remodeling and can acquire BAT-like, or "beige," characteristics upon appropriate stimulation, whereas gWAT is generally less prone to browning and acquiring a thermogenic phenotype (Villarroya et al., 2018).
Consistent with established literature, we have detected that scWAT successfully acquires BAT genetic characteristics, with significant upregulation of the transcriptional regulator *Prdm16* following cold exposure (Figure 9.A), reflecting its capacity for adaptive thermogenic programming (Seale et al., 2011). Despite the notion that visceral depots are less responsive, we also detected significant induction of several thermogenic genes (*Ucp1, Cidea, Prdm16, Elovl3*) in gWAT upon Clenbuterol treatment (Figure 10.A), an observation that is uncommon and suggests that pharmacological $\beta_2$-adrenergic stimulation may elicit a previously underappreciated thermogenic response in gonadal WAT.

Although we observed high fold changes, those can be partially attributed to differences in baseline thermogenic gene expression: even when largely silenced, BAT depots maintain higher baseline levels of key thermogenic genes, so fold-changes are less pronounced when plotted (Figure 9.B and 10.B). Subcutaneous WAT depot, with low basal expression, therefore, displays relatively large change, even at smaller transcript abundance.

Nonetheless, the transcriptional change in pBAT exceeded that observed in both scWAT and gWAT by several orders of magnitude. This pattern suggests that, unlike WAT, which requires acute activation or external cues to initiate a thermogenic program, pBAT is transcriptionally "prepared" for thermogenic responses, reflecting a depot-specific preparedness for adaptive energy expenditure.

## 4.7 Limitations and considerations for future studies

This study provides valuable insights into the transcriptional profile of pBAT, however there are several limitations that should be considered for future studies.

Firstly, this study focused on transcriptional levels of thermogenic genes but did not extend to protein levels due to the project scope and limited availability of the sample. Future studies that measure both transcript abundance and corresponding protein levels will be important to validate and confirm functional relevance of our findings.

Second, differences in depot size and cellular composition could influence gene expression patterns and may not directly translate to thermogenic output *in vivo*.

Third, our sample size was relatively small (n=4). While sufficient to reveal clear fold-changes, a larger cohort would provide stronger evidence, capture inter-individual variation, and greater statistical power of the results.

Another technical limitation of this study is the absence of formal purity validation for the micro-dissected pBAT samples. While anatomical landmarks and careful dissection were used to avoid contamination from surrounding tissues (such as white adipose tissue, muscle, or vasculature), residual heterogeneity cannot be fully excluded. To address this issue future studies could incorporate post-dissection validation approaches, such as histological assessment, immunohistochemical staining for brown adipocyte markers (e.g. UCP1), or transcriptomic/proteomic profiling to confirm enrichment of brown adipose tissue-specific signatures. Additionally, single-cell RNA sequencing could be used to quantify the relative abundance of brown adipocytes alongside other resident cell populations, thereby identifying potential contamination or heterogeneity. Complementary spatial transcriptomic or proteomic approaches would preserve tissue architecture, allowing verification that brown adipocyte specific markers are spatially confined to the dissected region and not influenced by adjacent tissues. Together, these approaches would provide robust validation of sample purity and enhance confidence that observed molecular signatures are truly pBAT-specific rather than driven by mixed cell populations.

Finally, the translational implications of these findings require careful consideration, as rodent BAT depots are not absolutely aligned with human BAT, and further work is needed to determine whether human pBAT depots show similar genetic responsiveness.

As a follow-up to this study, we suggest several experiments that can be considered to test thermogenic competence of pBAT:

First, protein-level validation using immunoblotting, immunohistochemistry, and mitochondrial respiration assays would confirm whether the observed transcriptional changes translate into functional outcomes.

Secondly, it would be useful to broaden the transcriptional dataset with additional mitochondrial and thermogenesis-related genes, such as the $\beta_2$- and $\beta_3$-adrenergic receptors.

This would help determine whether pBAT and iBAT show similar expressions of the main adrenergic receptors, giving a clearer picture of how each depot might respond to sympathetic stimulation. We were able to see moderate upregulation of *Ucp1* and *Cidea* in pBAT following the Clenbuterol treatment. To understand whether this resulted from activation of $\beta_2$AR expressed on the sympathetic ganglia innervating the depot, we suggest assessing using qRT-PCR in both adipocytes and sympathetic neurons. Measuring the cAMP response to $\beta_2$AR agonist treatment in both adipocytes and sympathetic neurons would clarify whether this thermogenic induction results from direct $\beta_2$AR signaling within BAT or indirectly through neuronal activation.

At the systems level, *in vivo* metabolic studies employing indirect calorimetry, thermal imaging, and PET-CT would establish the physiological contribution of pBAT to whole-body energy expenditure. Together, these approaches would build upon the present findings and deepen our understanding of pBAT as a distinct and highly dynamic thermogenic depot.

# 5

# Conclusions

## Contents



## 5.1 Concluding remarks

This research provides novel insights into the physiological role of paravertebral brown adipose tissue depot, which hasn't yet been explored. Our hypothesis was that pBAT plays an important role in non-shivering thermogenesis and metabolic homeostasis in mammals, due to its proximity to sympathetic chain, and vital organs.

Interestingly, our results revealed high baseline expression of key thermogenic gene program in pBAT of thermoneutral mice. Moreover, this depot is sensitive to both environmental temperature cues and β-adrenergic activation. Comparing these gene expression trends in pBAT to other adipose tissue sites provided us with sufficient evidence that pBAT has a strong full thermogenic gene programming, which is robust and comparable to classic iBAT. Such sensitivity to sympathetic stimulation highlights the functional relevance of pBAT as a metabolically active thermogenic depot, supporting its role in systemic energy balance during acute cold challenge.

These observations support our view of pBAT being well genetically "primed" to support oxidative metabolism in response to environmental cues. From a larger perspective, this study highlights that paravertebral brown fat could potentially represent a functional human alternative to classical interscapular brown adipose depot (iBAT). This is particularly

important in the context of any future translational studies, since this depot, unlike iBAT, is found to persist in adulthood in humans.

Considering the existing knowledge gap that currently limits progress in this field, we believe that further studies should be carried out to understand nature and function of paravertebral brown fat. Such studies will enhance our understanding of physiological role of pBAT in mammals and potentially pave the way for the development of future BAT-targeting anti-obesity treatments.

# References

Bardsley, E.N., Davis, H., Buckler, K.J. and Paterson, D.J. (2018). Neurotransmitter Switching Coupled to β-Adrenergic Signaling in Sympathetic Neurons in Prehypertensive States. *Hypertension (Dallas, Tex. : 1979)*, [online] 71(6), pp.1226–1238. doi:https://doi.org/10.1161/HYPERTENSIONAHA.118.10844.

Bartness, T.J., Vaughan, C.H. and Song, C.K. (2010). Sympathetic and sensory innervation of brown adipose tissue. *International Journal of Obesity (2005)*, [online] 34 Suppl 1, pp.S36-42. doi:https://doi.org/10.1038/ijo.2010.182.

Bersoux, S., Byun, T.H., Chaliki, S.S. and Poole, K.G. (2017). Pharmacotherapy for obesity: What you need to know. *Cleveland Clinic Journal of Medicine*, 84(12), pp.951–958. doi:https://doi.org/10.3949/ccjm.84a.16094.

Betz, M.J. and Enerbäck, S. (2018). Targeting thermogenesis in brown fat and muscle to treat obesity and metabolic disease. *Nature Reviews Endocrinology*, [online] 14(2), pp.77–87. doi:https://doi.org/10.1038/nrendo.2017.132.

Birerdinc, A., Jarrar, M., Stotish, T., Randhawa, M. and Baranova, A. (2013). Manipulating molecular switches in brown adipocytes and their precursors: A therapeutic potential. *Progress in Lipid Research*, 52(1), pp.51–61. doi:https://doi.org/10.1016/j.plipres.2012.08.001.

Bjørndal, B., Burri, L., Staalesen, V., Skorve, J. and Berge, R.K. (2011). Different Adipose Depots: Their Role in the Development of Metabolic Syndrome and Mitochondrial Response to Hypolipidemic Agents. *Journal of Obesity*, [online] 2011, pp.1–15. doi:https://doi.org/10.1155/2011/490650.

Blondin, D.P., Nielsen, S., Kuipers, E.N., Severinsen, M.C., Jensen, V.H., Miard, S., Jespersen, N.Z., Kooijman, S., Boon, M.R., Fortin, M., Phoenix, S., Frisch, F., Guérin, B., Turcotte, É.E., Haman, F., Richard, D., Picard, F., Rensen, P.C.N., Scheele, C. and Carpentier, A.C. (2020). Human Brown Adipocyte Thermogenesis Is Driven by β2-AR Stimulation. *Cell Metabolism*, 32(2), pp.287-300.e7. doi:https://doi.org/10.1016/j.cmet.2020.07.005.

Cannon, B. and Nedergaard, J. (2004). Brown Adipose Tissue: Function and Physiological Significance. *Physiological Reviews*, [online] 84(1), pp.277–359. doi:https://doi.org/10.1152/physrev.00015.2003.

Carpentier, A.C., Blondin, D.P., Haman, F. and Richard, D. (2022). Brown Adipose Tissue—A Translational Perspective. *Endocrine Reviews*, 44(2). doi:https://doi.org/10.1210/endrev/bnac015.

Carpentier, A.C., Blondin, D.P., Virtanen, K.A., Richard, D., Haman, F. and Turcotte, É.E. (2018). Brown Adipose Tissue Energy Metabolism in Humans. *Frontiers in Endocrinology*, [online] 9. doi:https://doi.org/10.3389/fendo.2018.00447.

Cheng, C.-F., Ku, H.-C. and Lin, H. (2018). PGC-1α as a Pivotal Factor in Lipid and Metabolic Regulation. *International Journal of Molecular Sciences*, 19(11), p.3447. doi:https://doi.org/10.3390/ijms19113447.

Cheung, S.W., Sidarta-Oliveira, D., Yao, L., Zhu, Y., Sarker, G., Lundh, S., Morgan, D.A., Qu, J., Wilcox, S., Vladyslav Vyazovskiy, Paterson, D.J., Li, D., Kamal Rahmouni and Domingos, A.I. (2025). $\beta_2$AR Agonists Sustain Thermogenesis and Leanness via*Sympathofacilitation*. *bioRxiv (Cold Spring Harbor Laboratory)*. doi:https://doi.org/10.1101/2025.06.13.659468.

Cypess, A.M., Lehman, S., Williams, G., Tal, I., Rodman, D., Goldfine, A.B., Kuo, F.C., Palmer, E.L., Tseng, Y.-H., Doria, A., Kolodny, G.M. and Kahn, C.R. (2009). Identification and Importance of Brown Adipose Tissue in Adult Humans. *Obstetrical & Gynecological Survey*, 64(8), pp.519–520. doi:https://doi.org/10.1097/ogx.0b013e3181ac8aa2.

Díaz-Castro, F., Morselli, E. and Claret, M. (2024). Interplay between the brain and adipose tissue: a metabolic conversation. *EMBO reports*, [online] 25(12), pp.5277–5293. doi:https://doi.org/10.1038/s44319-024-00321-4.

Duerre, D.J. and Galmozzi, A. (2022). Deconstructing Adipose Tissue Heterogeneity One Cell at a Time. *Frontiers in Endocrinology*, 13. doi:https://doi.org/10.3389/fendo.2022.847291.

Enerbäck, S., Jacobsson, A., Simpson, E.M., Guerra, C., Yamashita, H., Harper, M.-E. and Kozak, L.P. (1997). Mice lacking mitochondrial uncoupling protein are cold-sensitive but not obese. *Nature*, [online] 387(6628), pp.90–94. doi:https://doi.org/10.1038/387090a0.

Fedorenko, A., Lishko, P.V. and Kirichok, Y. (2012). Mechanism of Fatty-Acid-Dependent UCP1 Uncoupling in Brown Fat Mitochondria. *Cell*, 151(2), pp.400–413. doi:https://doi.org/10.1016/j.cell.2012.09.010.

Fernandez-Marcos, P.J. and Auwerx, J. (2011). Regulation of PGC-1α, a nodal regulator of mitochondrial biogenesis. *The American Journal of Clinical Nutrition*, 93(4), pp.884S890S. doi:https://doi.org/10.3945/ajcn.110.001917.

Fitzgibbons, T.P., Kogan, S., Aouadi, M., Hendricks, G.M., Straubhaar, J. and Czech, M.P. (2011). Similarity of mouse perivascular and brown adipose tissues and their resistance to diet-induced inflammation. *American Journal of Physiology-Heart and Circulatory Physiology*, 301(4), pp.H1425–H1437. doi:https://doi.org/10.1152/ajpheart.00376.2011.

Gesta, S., Tseng, Y.-H. and Kahn, C.R. (2007). Developmental Origin of Fat: Tracking Obesity to Its Source. *Cell*, 131(2), pp.242–256. doi:https://doi.org/10.1016/j.cell.2007.10.004.

Gilsanz, V., Hu, H.H. and Kajimura, S. (2013). Relevance of brown adipose tissue in infancy and adolescence. *Pediatric research*, [online] 73(1), pp.3–9. doi:https://doi.org/10.1038/pr.2012.141.

González-García, I., Milbank, E., Martinez-Ordoñez, A., Diéguez, C., López, M. and Contreras, C. (2019). HYPOTHesizing about central comBAT against obesity. *Journal of Physiology and Biochemistry*, 76(2), pp.193–211. doi:https://doi.org/10.1007/s13105-019-00719-y.

Grogan, A., Lucero, E.Y., Jiang, H. and Rockman, H.A. (2022). Pathophysiology and pharmacology of G protein-coupled receptors in the heart. *Cardiovascular Research*. doi:https://doi.org/10.1093/cvr/cvac171.

Grundlingh, J., Dargan, P.I., El-Zanfaly, M. and Wood, D.M. (2011). 2,4-dinitrophenol (DNP): a weight loss agent with significant acute toxicity and risk of death. *Journal of*

*medical toxicology : official journal of the American College of Medical Toxicology*, [online] 7(3), pp.205–12. doi:https://doi.org/10.1007/s13181-011-0162-6.

Guerra, C., Koza, R.A., Yamashita, H., Walsh, K. and Kozak, L.P. (1998). Emergence of brown adipocytes in white fat in mice is under genetic control. Effects on body weight and adiposity. *Journal of Clinical Investigation*, 102(2), pp.412–420. doi:https://doi.org/10.1172/jci3155.

Heaton, J.M. (1972). The distribution of brown adipose tissue in the human. *PubMed*, 112(Pt 1), pp.35–9.

Hertzman, A.B. (1959). Vasomotor Regulation of Cutaneous Circulation. *Physiological Reviews*, 39(2), pp.280–306. doi:https://doi.org/10.1152/physrev.1959.39.2.280.

Himms-Hagen, J. (1984). Nonshivering thermogenesis. *Brain research bulletin*, [online] 12(2), pp.151–60. doi:https://doi.org/10.1016/0361-9230(84)90183-7.

Jash, S., Banerjee, S., Lee, M.-J., Farmer, S.R. and Puri, V. (2019). CIDEA Transcriptionally Regulates UCP1 for Britening and Thermogenesis in Human Fat Cells. *iScience*, [online] 20, pp.73–89. doi:https://doi.org/10.1016/j.isci.2019.09.011.

Kajimura, S., Seale, P. and Spiegelman, B.M. (2010). Transcriptional Control of Brown Fat Development. *Cell Metabolism*, 11(4), pp.257–262. doi:https://doi.org/10.1016/j.cmet.2010.03.005.

Kazak, L., Chouchani, E.T., Stavrovskaya, I.G., Lu, G.Z., Jedrychowski, M.P., Egan, D.F., Kumari, M., Kong, X., Erickson, B.K., Szpyt, J., Rosen, E.D., Murphy, M.P., Kristal, B.S., Gygi, S.P. and Spiegelman, B.M. (2017). UCP1 deficiency causes brown fat respiratory chain depletion and sensitizes mitochondria to calcium overload-induced dysfunction. *Proceedings of the National Academy of Sciences*, 114(30), pp.7981–7986. doi:https://doi.org/10.1073/pnas.1705406114.

Klingenspor, M. (2003). Cold-Induced Recruitment of Brown Adipose Tissue Thermogenesis. *Experimental Physiology*, 88(1), pp.141–148. doi:https://doi.org/10.1113/eph8802508.

Kolovos, P., Knoch, T.A., Grosveld, F.G., Cook, P.R. and Papantonis, A. (2012). Enhancers and silencers: an integrated and simple model for their function. *Epigenetics & Chromatin*, [online] 5(1), p.1. doi:https://doi.org/10.1186/1756-8935-5-1.

Lee, J.-E., Schmidt, H., Lai, B. and Ge, K. (2019). Transcriptional and Epigenomic Regulation of Adipogenesis. *Molecular and cellular biology*, [online] 39(11), pp.e00601-18. doi:https://doi.org/10.1128/MCB.00601-18.

Lee, P., Swarbrick, M.M. and Ho, K.K.Y. (2013). Brown Adipose Tissue in Adult Humans: A Metabolic Renaissance. *Endocrine Reviews*, 34(3), pp.413–438. doi:https://doi.org/10.1210/er.2012-1081.

Lefterova, M.I., Zhang, Y., Steger, D.J., Schupp, M., Schug, J., Cristancho, A., Feng, D., Zhuo, D., Stoeckert, C.J., Liu, X.S. and Lazar, M.A. (2008). PPARgamma and C/EBP factors orchestrate adipocyte biology via adjacent binding on a genome-wide scale. *Genes & Development*, [online] 22(21), pp.2941–2952. doi:https://doi.org/10.1101/gad.1709008.

Leitner, B.P., Huang, S., Brychta, R.J., Duckworth, C.J., Baskin, A.S., McGehee, S., Tal, I., Dieckmann, W., Gupta, G., Kolodny, G.M., Pacak, K., Herscovitch, P., Cypess, A.M. and Chen, K.Y. (2017a). Mapping of human brown adipose tissue in lean and obese young men. *Proceedings of the National Academy of Sciences of the United States of America*, [online] 114(32), pp.8649–8654. doi:https://doi.org/10.1073/pnas.1705287114.

Leitner, B.P., Huang, S., Brychta, R.J., Duckworth, C.J., Baskin, A.S., McGehee, S., Tal, I., Dieckmann, W., Gupta, G., Kolodny, G.M., Pacak, K., Herscovitch, P., Cypess, A.M. and Chen, K.Y. (2017b). Mapping of human brown adipose tissue in lean and obese young men. *Proceedings of the National Academy of Sciences*, 114(32), pp.8649–8654. doi:https://doi.org/10.1073/pnas.1705287114.

Li, Y., Ping, X., Zhang, Y., Li, G., Zhang, T., Chen, G., Ma, X., Wang, D. and Xu, L. (2021). Comparative Transcriptome Profiling of Cold Exposure and β3-AR Agonist CL316,243-Induced Browning of White Fat. *Frontiers in physiology*, [online] 12, p.667698. doi:https://doi.org/10.3389/fphys.2021.667698.

Lidell, M.E. (2018). Brown Adipose Tissue in Human Infants. *Brown Adipose Tissue*, 251, pp.107–123. doi:https://doi.org/10.1007/164_2018_118.

Lidell, M.E., Betz, M.J., Dahlqvist Leinhard, O., Heglind, M., Elander, L., Slawik, M., Mussack, T., Nilsson, D., Romu, T., Nuutila, P., Virtanen, K.A., Beuschlein, F., Persson, A., Borga, M. and Enerbäck, S. (2013). Evidence for two types of brown adipose tissue in humans. *Nature Medicine*, [online] 19(5), pp.631–634. doi:https://doi.org/10.1038/nm.3017.

Lidell, M.E., Seifert, E.L., Westergren, R., Mikael Heglind, Gowing, A., Sukonina, V., Zahra Arani, Itkonen, P., Wallin, S., Westberg, F., Fernandez-Rodriguez, J., Laakso, M., Nilsson, T., Peng, X.-R., Harper, M.-E. and Sven Enerbäck (2011). The Adipocyte-Expressed Forkhead Transcription Factor Foxc2 Regulates Metabolism Through Altered Mitochondrial Function. *Diabetes*, 60(2), pp.427–435. doi:https://doi.org/10.2337/db10-0409.

Liu, X., Zhang, Z., Song, Y., Xie, H. and Dong, M. (2023). An update on brown adipose tissue and obesity intervention: Function, regulation and therapeutic implications. *Frontiers in Endocrinology*, 13. doi:https://doi.org/10.3389/fendo.2022.1065263.

Lockie, S.H., Stefanidis, A., Oldfield, B.J. and Perez-Tilve, D. (2013). Brown adipose tissue thermogenesis in the resistance to and reversal of obesity. *Adipocyte*, 2(4), pp.196–200. doi:https://doi.org/10.4161/adip.25417.

Luo, L. and Liu, M. (2016). Adipose tissue in control of metabolism. *The Journal of endocrinology*, [online] 231(3), pp.R77–R99. doi:https://doi.org/10.1530/JOE-16-0211.

Lynes, M.D. and Tseng, Y.-H. (2018). Deciphering adipose tissue heterogeneity. *Annals of the New York Academy of Sciences*, [online] 1411(1), pp.5–20. doi:https://doi.org/10.1111/nyas.13398.

Mahú, I., Barateiro, A., Rial-Pensado, E., Martinéz-Sánchez, N., Vaz, S.H., Cal, P.M.S.D., Jenkins, B., Rodrigues, T., Cordeiro, C., Costa, M.F., Mendes, R., Seixas, E., Pereira, M.M.A., Kubasova, N., Gres, V., Morris, I., Temporão, C., Olivares, M., Sanz, Y. and Koulman, A. (2020). Brain-Sparing Sympathofacilitators Mitigate Obesity without Adverse Cardiovascular Effects. *Cell Metabolism*, 31(6), pp.1120-1135.e7. doi:https://doi.org/10.1016/j.cmet.2020.04.013.

Mandarim-de-Lacerda, C.A., del Sol, M., Vásquez, B. and Aguila, M.B. (2021). Mice as an Animal Model for the Study of Adipose Tissue and Obesity. *International Journal of Morphology*, 39(6), pp.1521–1528. doi:https://doi.org/10.4067/s0717-95022021000601521.

Martínez-Sánchez, N., Moreno-Navarrete, J.M., Contreras, C., Rial-Pensado, E., Fernø, J., Nogueiras, R., Diéguez, C., Fernández-Real, J.-M. and López, M. (2017). Thyroid hormones induce browning of white fat. *Journal of Endocrinology*, 232(2), pp.351–362. doi:https://doi.org/10.1530/joe-16-0425.

Morrison, S., F. (2011). Central neural pathways for thermoregulation. *Frontiers in Bioscience*, [online] 16(1), p.74. doi:https://doi.org/10.2741/3677.

Mota-Rojas, D., Titto, C.G., Orihuela, A., Martínez-Burnes, J., Gómez-Prado, J., Torres-Bernal, F., Flores-Padilla, K., Carvajal-de la Fuente, V. and Wang, D. (2021). Physiological and Behavioral Mechanisms of Thermoregulation in Mammals. *Animals*, 11(6), p.1733. doi:https://doi.org/10.3390/ani11061733.

Mottillo, E.P., Balasubramanian, P., Lee, Y.-H., Weng, C., Kershaw, E.E. and Granneman, J.G. (2014). Coupling of lipolysis and de novo lipogenesis in brown, beige, and white adipose tissues during chronic β3-adrenergic receptor activation. *Journal of Lipid Research*, 55(11), pp.2276–2286. doi:https://doi.org/10.1194/jlr.m050005.

Murano, I., Barbatelli, G., Giordano, A. and Cinti, S. (2009). Noradrenergic parenchymal nerve fiber branching after cold acclimatisation correlates with brown adipocyte density in mouse adipose organ. *Journal of Anatomy*, 214(1), pp.171–178. doi:https://doi.org/10.1111/j.1469-7580.2008.01001.x.

Nedergaard, J., Bengtsson, T. and Cannon, B. (2007). Unexpected evidence for active brown adipose tissue in adult humans. *American Journal of Physiology-Endocrinology and Metabolism*, 293(2), pp.E444–E452. doi:https://doi.org/10.1152/ajpendo.00691.2006.

Nic-Can, G.I., Rodas-Junco, B.A., Carrillo-Cocom, L.M., Zepeda-Pedreguera, A., Peñaloza-Cuevas, R., Aguilar-Ayala, F.J. and Rojas-Herrera, R.A. (2019). Epigenetic Regulation of Adipogenic Differentiation by Histone Lysine Demethylation. *International Journal of Molecular Sciences*, 20(16), p.3918. doi:https://doi.org/10.3390/ijms20163918.

Nicholls, D.G. and Locke, R.M. (1984). Thermogenic mechanisms in brown fat. *Physiological Reviews*, 64(1), pp.1–64. doi:https://doi.org/10.1152/physrev.1984.64.1.1.

Oelkrug, R., Polymeropoulos, E.T. and Jastroch, M. (2015). Brown adipose tissue: physiological function and evolutionary significance. *Journal of Comparative Physiology B*, 185(6), pp.587–606. doi:https://doi.org/10.1007/s00360-015-0907-7.

Oguri, Y. and Kajimura, S. (2019). Cellular heterogeneity in brown adipose tissue. *Journal of Clinical Investigation*, 130(1), pp.65–67. doi:https://doi.org/10.1172/jci133786.

Okamatsu-Ogura, Y., Kuroda, M., Tsutsumi, R., Tsubota, A., Saito, M., Kimura, K. and Sakaue, H. (2020). UCP1-dependent and UCP1-independent metabolic changes induced by acute cold exposure in brown adipose tissue of mice. *Metabolism*, 113, p.154396. doi:https://doi.org/10.1016/j.metabol.2020.154396.

Orava, J., Nuutila, P., Lidell, Martin E., Oikonen, V., Noponen, T., Viljanen, T., Scheinin, M., Taittonen, M., Niemi, T., Enerbäck, S. and Virtanen, Kirsi A. (2011). Different Metabolic Responses of Human Brown Adipose Tissue to Activation by Cold and Insulin. *Cell Metabolism*, 14(2), pp.272–279. doi:https://doi.org/10.1016/j.cmet.2011.06.012.

Othman Abu Shelbayeh, Tasnim Arroum, Morris, S. and Busch, K.B. (2023). PGC-1α Is a Master Regulator of Mitochondrial Lifecycle and ROS Stress Response. *Antioxidants*, 12(5), pp.1075–1075. doi:https://doi.org/10.3390/antiox12051075.

Ouellet, V., Labbé, S.M., Blondin, D.P., Phoenix, S., Guérin, B., Haman, F., Turcotte, E.E., Richard, D. and Carpentier, A.C. (2012). Brown adipose tissue oxidative metabolism contributes to energy expenditure during acute cold exposure in humans. *Journal of Clinical Investigation*, 122(2), pp.545–552. doi:https://doi.org/10.1172/jci60433.

Palou, A., Picó, C., Bonet, M.Luisa. and Oliver, P. (1998). The uncoupling protein, thermogenin. *The International Journal of Biochemistry & Cell Biology*, [online] 30(1), pp.7–11. doi:https://doi.org/10.1016/s1357-2725(97)00065-4.

Park, A. (2014). Distinction of white, beige and brown adipocytes derived from mesenchymal stem cells. *World Journal of Stem Cells*, 6(1), p.33. doi:https://doi.org/10.4252/wjsc.v6.i1.33.

Puigserver, P., Wu, Z., Park, C.W., Graves, R., Wright, M. and Spiegelman, B.M. (1998). A Cold-Inducible Coactivator of Nuclear Receptors Linked to Adaptive Thermogenesis. *Cell*, 92(6), pp.829–839. doi:https://doi.org/10.1016/s0092-8674(00)81410-5.

Qin, H., Yadav, R., Basse, A.L., Petersen, S., Si Brask Sonne, Rasmussen, S., Zhu, Q., Lu, Z., Wang, J., Audouze, K., Gupta, R., Madsen, L., Kristiansen, K. and Hansen, J.B. (2015). Transcriptome profiling of brown adipose tissue during cold exposure reveals extensive regulation of glucose metabolism. *American Journal of Physiology-endocrinology and Metabolism*, 308(5), pp.E380–E392. doi:https://doi.org/10.1152/ajpendo.00277.2014.

Raiko, J., Orava, J., Savisto, N. and Virtanen, K.A. (2020). High Brown Fat Activity Correlates With Cardiovascular Risk Factor Levels Cross-Sectionally and Subclinical Atherosclerosis at 5-Year Follow-Up. *Arteriosclerosis, Thrombosis, and Vascular Biology*, 40(5), pp.1289–1295. doi:https://doi.org/10.1161/atvbaha.119.313806.

Ricquier, D. (2011). Uncoupling Protein 1 of Brown Adipocytes, the Only Uncoupler: A Historical Perspective. *Frontiers in Endocrinology*, 2. doi:https://doi.org/10.3389/fendo.2011.00085.

Ricquier, D. and Bouillaud, F. (2000). Mitochondrial uncoupling proteins: from mitochondria to the regulation of energy balance. *The Journal of Physiology*, 529(1), pp.3–10. doi:https://doi.org/10.1111/j.1469-7793.2000.00003.x.

Rosen, E.D. and Spiegelman, B.M. (2000). Molecular Regulation of Adipogenesis. *Annual Review of Cell and Developmental Biology*, 16(1), pp.145–171. doi:https://doi.org/10.1146/annurev.cellbio.16.1.145.

Rothwell, N.J. and Stock, M.J. (1979). A role for brown adipose tissue in diet-induced thermogenesis. *Nature*, [online] 281(5726), pp.31–35. doi:https://doi.org/10.1038/281031a0.

Sacks, H. and Symonds, M.E. (2013). Anatomical Locations of Human Brown Adipose Tissue: Functional Relevance and Implications in Obesity and Type 2 Diabetes. *Diabetes*, 62(6), pp.1783–1790. doi:https://doi.org/10.2337/db12-1430.

Saito, M. (2013). Brown Adipose Tissue as a Regulator of Energy Expenditure and Body Fat in Humans. *Diabetes & Metabolism Journal*, 37(1), p.22. doi:https://doi.org/10.4093/dmj.2013.37.1.22.

Saito, M., Matsushita, M., Yoneshiro, T. and Okamatsu-Ogura, Y. (2020). Brown Adipose Tissue, Diet-Induced Thermogenesis, and Thermogenic Food Ingredients: From Mice to Men. *Frontiers in Endocrinology*, 11. doi:https://doi.org/10.3389/fendo.2020.00222.

Saito, M., Okamatsu-Ogura, Y., Matsushita, M., Watanabe, K., Yoneshiro, T., Nio-Kobayashi, J., Iwanaga, T., Miyagawa, M., Kameya, T., Nakada, K., Kawai, Y. and Tsujisaki, M. (2009). High incidence of metabolically active brown adipose tissue in healthy adult humans: effects of cold exposure and adiposity. *Diabetes*, [online] 58(7), pp.1526–1531. doi:https://doi.org/10.2337/db09-0530.

Sanchez-Gurmaches, J. and Guertin, D.A. (2014). Adipocyte lineages: Tracing back the origins of fat. *Biochimica et Biophysica Acta (BBA) - Molecular Basis of Disease*, 1842(3), pp.340–351. doi:https://doi.org/10.1016/j.bbadis.2013.05.027.

Seale, P. (2015). Transcriptional Regulatory Circuits Controlling Brown Fat Development and Activation. *Diabetes*, [online] 64(7), pp.2369–2375. doi:https://doi.org/10.2337/db15-0203.

Seale, P., Conroe, H.M., Estall, J., Kajimura, S., Frontini, A., Ishibashi, J., Cohen, P., Cinti, S. and Spiegelman, B.M. (2011). Prdm16 determines the thermogenic program of subcutaneous white adipose tissue in mice. *Journal of Clinical Investigation*, 121(1), pp.96–105. doi:https://doi.org/10.1172/jci44271.

Shinsuke Nirengi and Stanford, K.I. (2023). Brown adipose tissue and aging: A potential role for exercise. *Experimental Gerontology*, 178, pp.112218–112218. doi:https://doi.org/10.1016/j.exger.2023.112218.

Sidossis, L. and Kajimura, S. (2015). Brown and beige fat in humans: thermogenic adipocytes that control energy and glucose homeostasis. *Journal of Clinical Investigation*, 125(2), pp.478–486. doi:https://doi.org/10.1172/jci78362.

Singh, R., Barrios, A., Dirakvand, G. and Pervin, S. (2021). Human Brown Adipose Tissue and Metabolic Health: Potential for Therapeutic Avenues. *Cells*, [online] 10(11), p.3030. doi:https://doi.org/10.3390/cells10113030.

Smith, R.E. (1964). Thermoregulatory and Adaptive Behavior of Brown Adipose Tissue. *Science*, [online] 146(3652), pp.1686–1689. doi:https://doi.org/10.1126/science.146.3652.1686.

Song, A., Dai, W., Min Jee Jang, Medrano, L., Li, Z., Zhao, H., Shao, M., Tan, J., Li, A., Ning, T., Miller, M.M., Armstrong, B., Huss, J.M., Zhu, Y., Liu, Y., Gradinaru, V., Wu, X., Jiang, L., Scherer, P.E. and Wang, Q.A. (2019). Low- and high-thermogenic brown adipocyte subpopulations coexist in murine adipose tissue. *Journal of Clinical Investigation*, 130(1), pp.247–257. doi:https://doi.org/10.1172/jci129167.

Spaethling, J.M., Sanchez-Alavez, M., Lee, J., Xia, F.C., Dueck, H., Wang, W., Fisher, S.A., Sul, J., Seale, P., Kim, J., Bartfai, T. and Eberwine, J. (2015). Single-cell transcriptomics and functional target validation of brown adipocytes show their complex roles in metabolic homeostasis. *The FASEB Journal*, 30(1), pp.81–92. doi:https://doi.org/10.1096/fj.15-273797.

Straat, M.E., Hoekx, C.A., Velden, van, Pereira, M., Dumont, L., Blondin, D.P., Boon, M.R., Borja Martinez-Tellez and Rensen, P.C.N. (2023). Stimulation of the beta-2-adrenergic receptor with salbutamol activates human brown adipose tissue. 4(2), pp.100942–100942. doi:https://doi.org/10.1016/j.xcrm.2023.100942.

Symonds, M.E., Pope, M. and Budge, H. (2015). The Ontogeny of Brown Adipose Tissue. *Annual Review of Nutrition*, 35(1), pp.295–320. doi:https://doi.org/10.1146/annurev-nutr-071813-105330.

van der Lans, A.A.J.J., Wierts, R., Vosselman, M.J., Schrauwen, P., Brans, B. and van Marken Lichtenbelt, W.D. (2014). Cold-activated brown adipose tissue in human adults: methodological issues. *American Journal of Physiology-Regulatory, Integrative and Comparative Physiology*, 307(2), pp.R103–R113. doi:https://doi.org/10.1152/ajpregu.00021.2014.

van Marken Lichtenbelt, W.D., Vanhommerig, J.W., Smulders, N.M., Drossaerts, J.M.A.F.L., Kemerink, G.J., Bouvy, N.D., Schrauwen, P. and Teule, G.J.J. (2009). Cold-Activated Brown Adipose Tissue in Healthy Men. *New England Journal of Medicine*, 360(15), pp.1500–1508. doi:https://doi.org/10.1056/nejmoa0808718.

Vegiopoulos, A. and Herzig, S. (2007). Glucocorticoids, metabolism and metabolic diseases. *Molecular and Cellular Endocrinology*, 275(1-2), pp.43–61. doi:https://doi.org/10.1016/j.mce.2007.05.015.

Vidal, P. and Stanford, K.I. (2020). Exercise-Induced Adaptations to Adipose Tissue Thermogenesis. *Frontiers in Endocrinology*, 11. doi:https://doi.org/10.3389/fendo.2020.00270.

Villarroya, F., Cereijo, R., Gavaldà-Navarro, A., Villarroya, J. and Giralt, M. (2018). Inflammation of brown/beige adipose tissues in obesity and metabolic disease. *Journal of Internal Medicine*, [online] 284(5), pp.492–504. doi:https://doi.org/10.1111/joim.12803.

Virtanen, K.A., Lidell, M.E., Orava, J., Heglind, M., Westergren, R., Niemi, T., Taittonen, M., Laine, J., Savisto, N.-J., Enerbäck, S. and Nuutila, P. (2009). Functional Brown Adipose Tissue in Healthy Adults. *New England Journal of Medicine*, 360(15), pp.1518–1525. doi:https://doi.org/10.1056/nejmoa0808949.

Wang, Q., Liu, Y., Xu, Y., Jin, Y., Wu, J. and Ren, Z. (2022). Comparative transcriptome and Lipidome analyses suggest a lipid droplet-specific response to heat exposure of brown adipose tissue in normal and obese mice. *Life Sciences*, [online] 299, p.120540. doi:https://doi.org/10.1016/j.lfs.2022.120540.

Westerberg, R., Månsson, J.-E., Golozoubova, V., Shabalina, I.G., Backlund, E.C., Tvrdik, P., Retterstøl, K., Capecchi, M.R. and Jacobsson, A. (2006). ELOVL3 Is an Important Component for Early Onset of Lipid Recruitment in Brown Adipose Tissue. *Journal of Biological Chemistry*, 281(8), pp.4958–4968. doi:https://doi.org/10.1074/jbc.m511588200.

Wu, J., Boström, P., Sparks, Lauren M., Ye, L., Choi, J., Giang, A.-H., Khandekar, M., Virtanen, Kirsi A., Nuutila, P., Schaart, G., Huang, K., Tu, H., van Marken Lichtenbelt, Wouter D., Hoeks, J., Enerbäck, S., Schrauwen, P. and Spiegelman, Bruce M. (2012). Beige

Adipocytes Are a Distinct Type of Thermogenic Fat Cell in Mouse and Human. *Cell*, [online] 150(2), pp.366–376. doi:https://doi.org/10.1016/j.cell.2012.05.016.

Wu, J., Cohen, P. and Spiegelman, B.M. (2013). Adaptive thermogenesis in adipocytes: Is beige the new brown? *Genes & Development*, 27(3), pp.234–250. doi:https://doi.org/10.1101/gad.211649.112.

Xue, R., Lynes, M.D., Dreyfuss, J.M., Shamsi, F., Schulz, T.J., Zhang, H., Huang, T.L., Townsend, K.L., Li, Y., Takahashi, H., Weiner, L.S., White, A.P., Lynes, M.S., Rubin, L.L., Goodyear, L.J., Cypess, A.M. and Tseng, Y.-H. (2015). Clonal analyses and gene profiling identify genetic biomarkers of the thermogenic potential of human brown and white preadipocytes. *Nature Medicine*, [online] 21(7), pp.760–768. doi:https://doi.org/10.1038/nm.3881.

Zhu, Q., Glazier, B.J., Hinkel, B.C., Cao, J., Liu, L., Liang, C. and Shi, H. (2019). Neuroendocrine Regulation of Energy Metabolism Involving Different Types of Adipose Tissues. *International Journal of Molecular Sciences*, [online] 20(11), p.2707. doi:https://doi.org/10.3390/ijms20112707.

Zwick, R.K., Guerrero-Juarez, C.F., Horsley, V. and Plikus, M.V. (2018). Anatomical, physiological and functional diversity of adipose tissue. *Cell metabolism*, [online] 27(1), pp.68–83. doi:https://doi.org/10.1016/j.cmet.2017.12.002.

.